Five thermodynamic describers for addressing serendipity in the self-assembly of polynuclear complexes in solution†

Claude Piguet*

Received 7th April 2010, Accepted 28th May 2010
DOI: 10.1039/c0cc00811g

The thermodynamic self-assembly of any metallo-supramolecular complex $[M_{pm}L_{pn}]$ in solution can be dissected into five additive free energy contributions. According to a hierarchical energetic order, the two microscopic describers f_{inter} and f_{intra}, which refer to the hetero-component metal–ligand connections, bring the main driving forces to the complexation process. Combined with the statistical factor ω of the self-assembly, which measures the changes in intrinsic rotational entropies accompanying the complexation process, these three parameters provide a satisfying description of the statistical binding leading to $[M_{pm}L_{pn}]$ in solution. Deviations from statistics, *i.e.* cooperativity, has then two different origins. Firstly, the preorganization controlling the intramolecular connection events may vary along the assembly process, thus affecting f_{intra}. Secondly, the homo-component interactions brought by the specific location of the different components in the final assembly (M···M interactions: $\Delta E^{M,M}$, and L···L interactions: $\Delta E^{L,L}$), may additionally contribute to the total free energy change and affect f_{inter}. Beyond the determination of quantitative experimental values for these five parameters operating in various metal-containing assemblies, considerable efforts have been focused on their physico–chemical origins, with the ultimate goal of unravelling their chemical design. In this Feature Article, the bases are first considered leading to the emergence of the free additive thermodynamic model in metallo-supramolecular chemistry. A tutorial discussion of the current level of understanding of each microscopic thermodynamic describer follows, together with some selected practical applications in the field of polynuclear d-block and f-block complexes.

Department of Inorganic, Analytical and Applied Chemistry, University of Geneva, 30 quai Ernest Ansermet, CH-1211 Geneva 4. Claude. E-mail: Piguet@unige.ch; Fax: (41 22) 379 6830; Tel: (41 22) 379 6034

† Dedicated to Professor Gianfranco Ercolani for his seminal contributions to this field

Claude Piguet

Claude Piguet earned a PhD degree in 1989 in the field of biomimetic copper-dioxygen complexes. After postdoctoral periods in the groups of professors J.-M. Lehn, A. F. Williams, and J.-C. G. Bünzli, he initiated research projects in the field of lanthanide supramolecular chemistry. He received the Werner Medal of the New Swiss Chemical Society (1995) and was appointed in as a full professor of inorganic chemistry at the University of Geneva (1999). He has co-authored more than 150 scientific articles addressing various aspects of basic chemistry. In 2009, he was awarded the Lecoq de Boisbaudran Senior Award from the European Rare Earth Society, and taught as an invited professor at the Ecole Normale Supérieure in Paris.

1. Introduction: multi-valency in coordination chemistry

At the turn of the nineteenth century, Werner[1] indeed realized that the controversial maximum valency of the carbon atom, eventually fixed to four by Abegg[2] and Lewis,[3] is not a general trend, and that many other possibilities (in modern language, other coordination numbers, *CN*) can be found for the various elements of the periodic table. With this concept in mind, coordination chemistry rapidly evolved toward a well-recognized part of chemistry dealing with variable coordination numbers (*CN* = 2–6), but clearly dominated by octahedral geometry thanks to the discovery of the exceptional stabilities and analytical versatilities of the complexes formed between bivalent and trivalent s-, p- and d-block cations with multidentate polyaminocarboxylates, such as 2,2′,2″-nitrilotriacetic acid (NTA) or 2,2′,2″,2‴-(ethane-1,2-diyldinitrilo)tetraacetic acid (EDTA), Fig. 1a).[4,5] Interestingly, the combination of these polyaminocarboxylates with cerium(III) and yttrium(III) by Schwarzenbach himself during the early sixties casted doubt about his comfortable six-coordinate theory of EDTA complexes. The publication by Hoard and co-workers in 1965 of the crystal structure of $NH_4Lu(EDTA)\cdot 8H_2O$, whereby Lu^{III} is nine-coordinated, unambiguously extended the conceivable valencies beyond six for large cations.[6] The recognition that large valencies may bring some extra stabilization for specific metallic centres stimulated interest

for the related design of multidentate ligands, in which the connections of several donor atoms belonging to the same ligand also contribute to stabilize the final assemblies.[7] The underlying concept of multi-valency, which can be defined as the connection of two microscopic components (organic molecules, metallic cations, inorganic anions, *etc.*) by using at least two concomitant interactions, had a parallel rich and fruitful career in macromolecular chemistry, in polymer chemistry and in biology.[8] Some improvements in stability, specificity and selectivity usually result from the judicious integration of several (sometimes different) convergent interactions contributing to the same connection event, in line with the concept of 'molecular recognition'.[9] The accidental[10] or deliberate[11] syntheses of hollow macro(poly)cyclic receptors during the early 1970s re-focused an intense activity on the selective complexation of small cationic, neutral or anionic guests by sophisticated multidentate hosts, with some emphasis on the reaction mechanisms and the thermodynamic balances (Fig. 1b and c). The report by Lehn and co-workers of the first planned self-assembled trinuclear helicate in 1987 (Fig. 1d),[12] rapidly followed by the exploitation of the metal-induced helical twist by Sauvage and co-workers for the preparation of some unprecedented entangled ligand strands, strongly contribute to the recognition of classical metal–ligand dative bonds as new tools for producing complicate (supra)molecular objects (Fig. 2).[13]

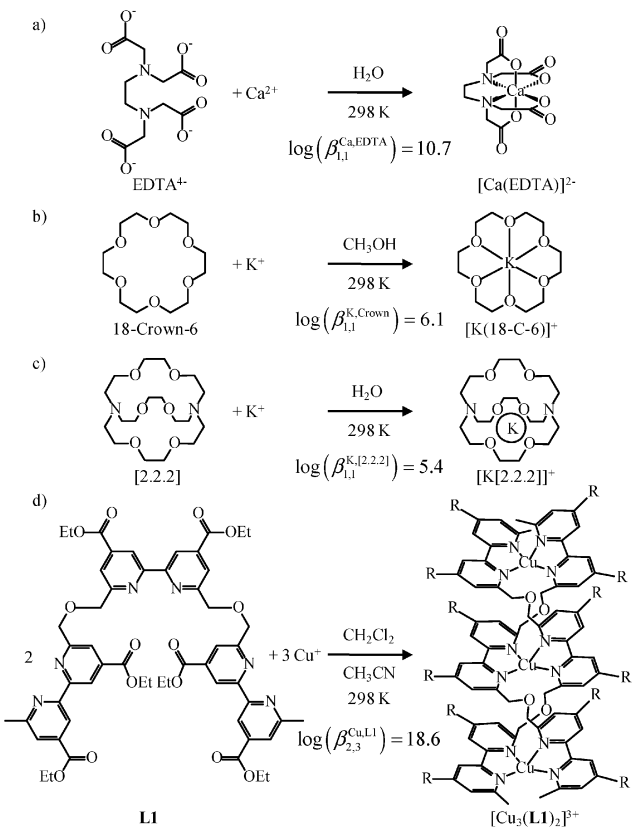

Fig. 1 The early steps of multi-valency in coordination and metallo-supramolecular chemistry showing the formation of (a) a chelate complex,[4] (b) a macrocyclic complex,[10,11] (c) a macrobicyclic complex[11] and (d) a self-assembled complex.[12]

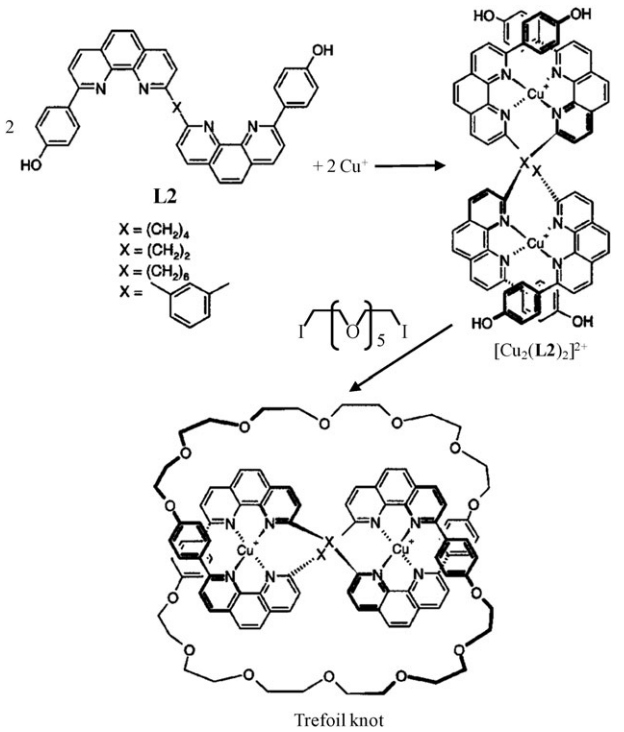

Fig. 2 Synthesis of the first metal-templated trefoil knots.[13]

Numerous chemists, previously active in coordination chemistry, joined the emerging field of metallo-supramolecular chemistry at the turn of the ninetieth. A plethora of aesthetically appealing and non-trivial combinations of metals and ligands were thus the subject of innumerable and remarkable reports during the last two decades, with the ultimate goal of discovering novel functions, properties or applications arising from the increased complexity produced by the considerable number of inter-connected components (Fig. 3).[14]

Surprisingly, the investigations of the fundamental kinetic and thermodynamic mechanisms leading to the formation of these challenging multi-component complexes remain scarce, despite noticeable initial inputs by Lehn, Albrecht-Gary and co-workers.[12b,15] According to a thermodynamic point of view, early investigators attempted to use the well-established protein-ligand model, combined with Scatchard or Hill plots for rationalizing the complicated connection processes operating in $[M_{pm}L_{pn}]$.[12b,15] However, in 2003, Ercolani judiciously pointed out that the assembly of metallo-supramolecular complexes indeed involves the combination of both inter- and intramolecular hetero-component metal–ligand connections,[16] which prevents the use of Scatchard or Hill plots for unravelling cooperativity.[17] In his seminal paper, Ercolani eventually demonstrated that the self-assembly of famous Lehn's double-stranded helicate $[Cu_3(\mathbf{L1})_2]^{3+}$ (Fig. 1d) follows a statistical algorithm, once inter- and intramolecular Cu–ligand connections have been satisfyingly modeled.[16a] A slightly refined version of this basic approach[18] was then successfully applied for unravelling the stabilities of standard coordination complexes,[19] linear helicates[18] and polynuclear two-dimensional clusters.[20] Following the same strategy, Hunter and co-workers

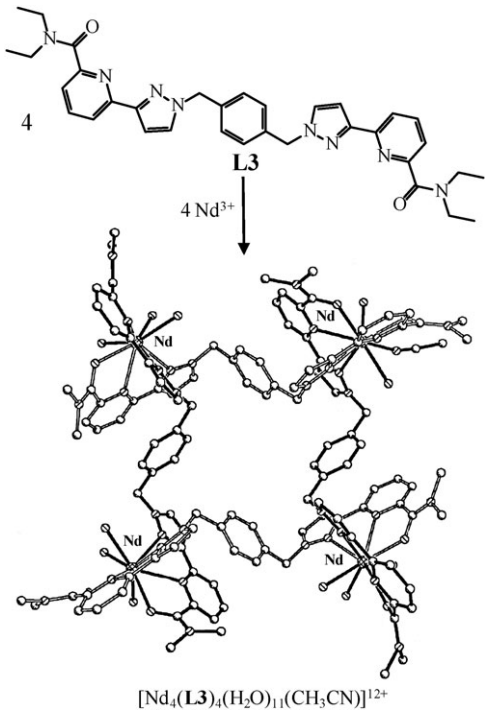

Fig. 3 Formation of a sophisticated tetranuclear unsaturated single-stranded lanthanide helicate.[1q4q]

extended its potential for quantitatively highlighting the advantages of the formation of intramolecular hydrogen bonds between preorganized multivalent H-donor and H-acceptor molecules.[21] The fitted microscopic thermodynamic parameters usually shed some light on the relative importance of the contribution of each microscopic describers to the global free energy change responsible for the self-assembly. However, the physical origin and the deliberate chemical tuning of these microscopic thermodynamic parameters remain often elusive. Four years ago, the thermodynamic concepts leading to the emergence of the free additive model in coordination chemistry was reviewed.[22] In this second feature article, justification is first provided for the use of five microscopic thermodynamic describers for the modeling of any self-assembly process involving two different components. A tutorial discussion addressing the physical origins and the potential chemical tuning (*i.e.* structure–properties relationship) of these thermodynamic describers follows, with a special emphasis on simple practical applications and interpretations.

2. The thermodynamic additive free energy model

The formation of any supramolecular complex made from two building blocks (**M** = metal, **L** = ligand) can be described with equilibrium (1).

$$pm\ \mathbf{M} + pn\ \mathbf{L} \rightleftharpoons [\mathbf{M}_{pm}\mathbf{L}_{pn}]\ \beta^{\mathbf{M},\mathbf{L}}_{pm,pn} \qquad (1)$$

The associated cumulative stability constant $\beta^{\mathbf{M},\mathbf{L}}_{pm,pn}$ is given in eqn (2), whereby each pair of parallel vertical lines refers to molar concentrations and c^{θ} is the reference molar concentration in the standard state.[7]

$$\beta^{\mathbf{M},\mathbf{L}}_{pm,pn} = \frac{(|[\mathbf{M}_{pm}\mathbf{L}_{pn}|/c^{\theta})}{(|\mathbf{M}|/c^{\theta})^{pm}(|\mathbf{L}|/c^{\theta})^{pn}} = \frac{|[\mathbf{M}_{pm}\mathbf{L}_{pn}|}{|\mathbf{M}|^{pm}|\mathbf{L}|^{pn}}(c^{\theta})^{(pm+pn-1)} \qquad (2)$$

The application of the van't Hoff isotherm $\Delta G^{0} = -RT\ln(\beta)$ gives eqn (3).

$$\Delta G^{\circ\,\mathbf{M},\mathbf{L}}_{pm,pn} = -RT\ln(\beta^{\mathbf{M},\mathbf{L}}_{pm,pn}) = -RT\ln\left(\frac{|[\mathbf{M}_{pm}\mathbf{L}_{pn}|}{|\mathbf{M}|^{pm}|\mathbf{L}|^{pn}}\right) - RT(pm+pn-1)\ln(c^{\theta}) \qquad (3)$$

Usually, chemists implicitely refer to the convenient one molar standard state (*i.e.* $c^{\theta} = 1$ M), and $\beta^{\mathbf{M},\mathbf{L}}_{pm,pn}$ can be experimentally estimated from standard speciations performed under thermodynamic equilibrium. This well-accepted reference standard state will obviously be adopted for the remainder of our discussions, but it is worth to keep in mind that (i) $\beta^{\mathbf{M},\mathbf{L}}_{pm,pn}$ has formally no units and (ii) the absolute entropy change $-T\Delta S^{\circ\mathbf{M},\mathbf{L}}_{pm,pn}$ contributing to $\Delta G^{\circ\mathbf{M},\mathbf{L}}_{pm,pn} = -RT\ln(\beta^{\mathbf{M},\mathbf{L}}_{pm,pn})$ (eqn (3)) depends on the choice of the reference standard state.[7] Assuming the principle of maximum site occupancy, the stoichiometry in the final complex $[\mathbf{M}_{pm}\mathbf{L}_{pn}]$ results from the connection of *pm* metals, each having *n* binding sites, with *pn* ligand, each having *m* binding sites.[16a] The final complex $[\mathbf{M}_{pm}\mathbf{L}_{pn}]$ thus contains $N = pm + pn$ components joined by $B = pmn$ connections, among which $N - 1 = pm + pn - 1$ are intermolecular and $B - (N - 1) = pmn - pm - pn + 1$ are intramolecular (Fig. 4).[16a]

Assigning the specific free energy contributions $\Delta g^{\mathbf{M},\mathbf{L}}_{\mathrm{inter}} = -RT\ln(f^{\mathbf{M},\mathbf{L}}_{\mathrm{inter}})$ and $\Delta g^{\mathbf{M},\mathbf{L}}_{\mathrm{intra}} = -RT\ln(f^{\mathbf{M},\mathbf{L}}_{\mathrm{intra}})$ to each type of hetero-component connection (including desolvation) leads to the original additive free energy model proposed by Ercolani (eqn (4)), which is transformed by using the van't Hoff isotherm into its compact formulation for modeling stability constants (eqn (5)).[16a]

$$\Delta G^{\circ\mathbf{M},\mathbf{L}}_{pm,pn} = -RT\ln(\omega^{\mathbf{M},\mathbf{L}}_{pm,pn}) - (pm + pn - 1)RT\ln(f^{\mathbf{M},\mathbf{L}}_{\mathrm{inter}}) - (pmn - pm - pn + 1)RT\ln(f^{\mathbf{M},\mathbf{L}}_{\mathrm{intra}}) \qquad (4)$$

$$\beta^{\mathbf{M},\mathbf{L}}_{pm,pn} = \omega^{\mathbf{M},\mathbf{L}}_{pm,pn}(f^{\mathbf{M},\mathbf{L}}_{\mathrm{inter}})^{pm+pn-1}(f^{\mathbf{M},\mathbf{L}}_{\mathrm{intra}})^{pmn-pm-pn+1} \qquad (5)$$

While $f^{\mathbf{M},\mathbf{L}}_{\mathrm{inter}}$ and $f^{\mathbf{M},\mathbf{L}}_{\mathrm{intra}}$ simply correspond to the absolute affinities of the binding site for the intermolecular, respectively intramolecular connection with the entering metal ion in terms of stability constants, $\omega^{\mathbf{M},\mathbf{L}}_{pm,pn}$ takes into account the pure statistical (*i.e.* entropic) contribution due to the change in the molecular rotational degeneracies occurring when the reactants are transformed into products.[24] Once the point groups of each partner contributing to the self-assembly are at hand, $\omega^{\mathbf{M},\mathbf{L}}_{pm,pn}$ can be easily *a priori* calculated with eqn (6) by

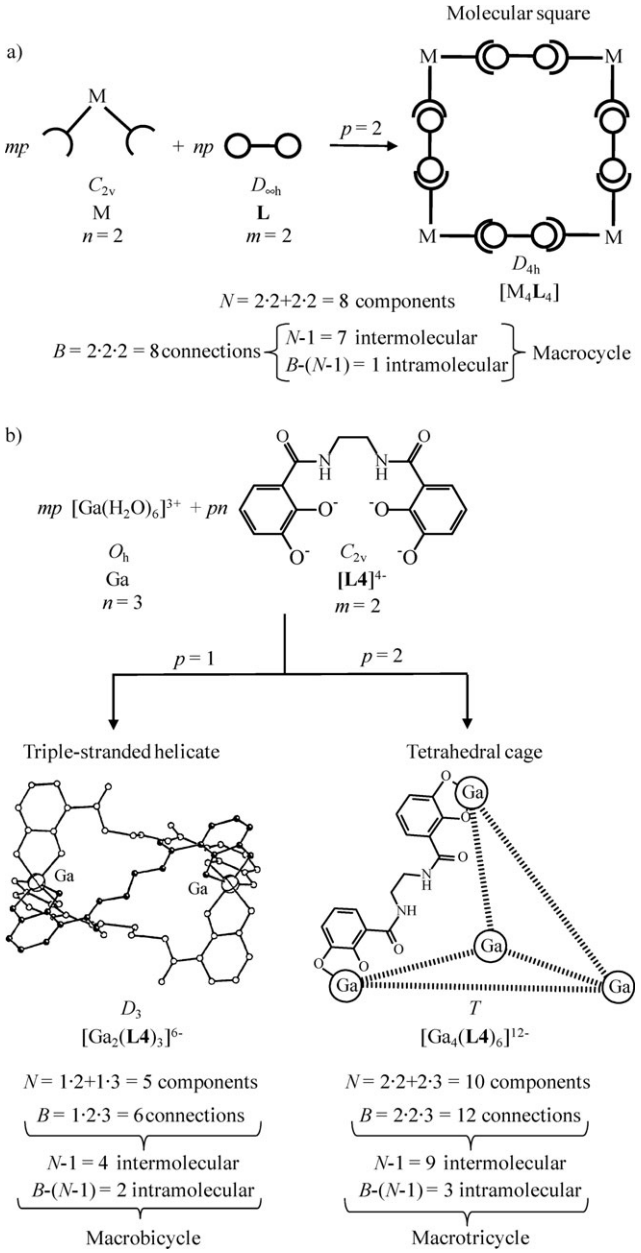

Fig. 4 (a) Cartoon and (b) experimental assemblies[23] illustrating the distribution of inter- and intramolecular hetero-component connections joining the $N = pm + pn$ components in the saturated final complexes $[M_{pm}L_{pn}]$. Note that each metal–ligand interaction is considered as a single connection point.

using their symmetry numbers σ_{tot}.[24] We will learn more about this method and the important consequences of $\omega_{pm,pn}^{M,L}$ on the thermodynamic programming of sophisticated assemblies in the next section.

$$\omega_{pm,pn}^{M,L} = \frac{(\sigma_{tot}^{M})^{pm}(\sigma_{tot}^{L})^{pn}}{(\sigma_{tot}^{M_{pm}L_{pn}})} \quad (6)$$

As an illustration of the remarkable simplicity of Ercolani's approach, lets apply eqn (5) for the modeling of equilibrium (7), which leads to the formation of the macrobicyclic triple-stranded helicate $[Ga_2(\mathbf{L4})_3]^{6-}$ shown in Fig. 4b.[23]

$$2\,[Ga(H_2O)_6]^{3+} + 3\,[\mathbf{L4}]^{4-} \rightleftharpoons [Ga_2(\mathbf{L4})_3]^{6-} + 12\,H_2O;\ \beta_{2,3}^{Ga,L4} \quad (7)$$

After calculation of the statistical factor $\omega_{2,3}^{Ga,L4} = 1536$ (see next section),[24] we find eqn (8), in which only two fitted microscopic parameters are required.

$$\beta_{2,3}^{Ga,L4} = 1536(f_{inter}^{Ga,L4})^4(f_{intra}^{Ga,L4})^2 \quad (8)$$

Assuming that the complexation process provides a sufficient amount of accessible stability constants characterizing the thermodynamic intermediates leading to the final complex, the self-assembly process is said to be non-cooperative if a single set of microscopic describers $f_{inter}^{M,L}$ and $f_{intra}^{M,L}$ satisfyingly reproduces the stability constant of each incriminated complex.[16a] Any deviations requiring an increase (respectively a decrease) of $f_{inter}^{M,L}$ and/or $f_{intra}^{M,L}$ accompanying the stepwise formation of the final assembly is attributed to positive (respectively negative) cooperativity. However, the variations of these two parameters in cooperative self-assembly processes are often difficult to correlate with a straightforward chemical interpretation of their origins. As a first step toward this goal, the well-known concept of effective concentration, experimentally given by the effective molarity, EM, is used for correlating $f_{inter}^{M,L}$ and $f_{intra}^{M,L}$ (eqn (9), and Fig. 5).[8,25]

$$f_{intra}^{M,L} = f_{inter}^{M,L}(EM/c^{\theta}) \quad (9)$$

EM has thus molar concentration unit[8,25] and its consequence on the free energy change depends of the choice of the reference standard state, a phenomenon at the origin of lively debates during the 1960s when attempting to define some absolute chelate effects in coordination chemistry.[7] Interestingly, the magnitude of EM,[7,26] and its dependence on the mean-square distance separating the donor atoms in a higly flexible ligand can be theoretically approached,[27] which allows some physico–chemical interpretations and predictions for $f_{intra}^{M,L}$, when $f_{inter}^{M,L}$ is at hand. In absence of ring strain ($\Delta H_{inter} = \Delta H_{intra}$), EM indeed corresponds to a purely entropic contribution measuring the advantage ($EM > 1$) or drawback ($EM < 1$) accompanying the formation of an intramolecular M–**L** connection (*i.e.* macrocyclization = formation of a chelate ring), with respect to the intermolecular association of the same metal with a second ligand, all reference states being fixed to $c^{\theta} = 1$ M (eqn (9) and Fig. 5). Mathematically speaking, the introduction of eqn (9) into eqn (5) gives eqn (10), in which $f_{inter}^{M,L}$, EM and $\omega_{pm,pn}^{M,L}$ are the microscopic thermodynamic describers modeling the stability of the self-assembled complex.

$$\beta_{pm,pn}^{M,L} = \omega_{pm,pn}^{M,L}(f_{inter}^{M,L})^{pmn}(EM_{pm,pn}^{M,L})^{pmn-pm-pn+1} \quad (10)$$

Since EM can be unambiguously assigned to preorganization, its invariability for the successive intramolecular hetero-component connections leading to the final self-assembled complex indicates a non-cooperative process, while its variation measures some changes in preorganization within the operation of the self-assembly process, and thus contributes to the global cooperativity.[28] The variation of $f_{inter}^{M,L}$ during the assembly process represents the second supply for cooperativity in

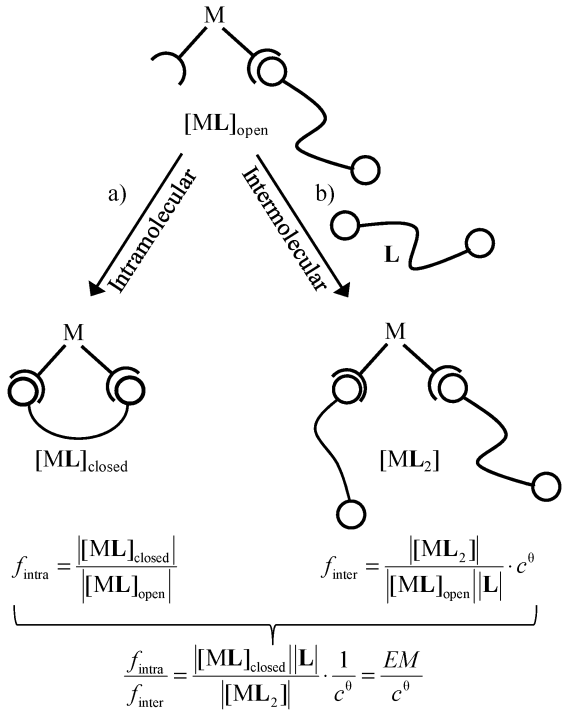

Fig. 5 Competition between (a) intermolecular and (b) intramolecular complexation processes in the formation of coordination complexes.[25]

Ercolani's model (eqn (10)), and its apparent change has been assigned to the operation of homo-component M···M or **L**···**L** interactions ($\Delta E^{M,M}$ and $\Delta E^{L,L}$) in $[M_{pm}\mathbf{L}_{pn}]$.[18] The explicit introduction of these perturbations as correcting Boltzmann factors $u^{M,M} = e^{-(\Delta E^{M,M}/RT)}$ and $u^{L,L} = e^{-(\Delta E^{L,L}/RT)}$ into eqn (10) gives eqn (11),[22] which contains five different microscopic thermodynamic describers.[29]

$$\beta^{M,L}_{pm,pn} = \omega^{M,L}_{pm,pn}(f^{M,L}_{inter})^{pmn}(EM^{M,L}_{pm,pn})^{pmn-pm-pn+1} \times \prod_i e^{-(\Delta E^{M,M}/RT)} \prod_i e^{-(\Delta E^{L,L}/RT)} \quad (11)$$

The total number of interligand and intermetallic interactions occuring in $[M_{pm}\mathbf{L}_{pn}]$ depends on the structural organization of the various components. Once the molecular structure is at hand, the number of intermetallic interactions are obtained by counting the number of possible different metallic pairs (through-space interactions), while the number of interligand interactions are taken as the number of possible different pairs of binding sites connected to the same metal (through-metal interactions).[18,22] Lets apply these definitions for the triple-stranded helicate $[Ga_2(\mathbf{L4})_3]^{6-}$ shown in Fig. 4b as a working example. We count only one intermetallic interaction (one possible Ga/Ga pair), but six interligand interactions because each Ga^{III} is bound to three bidentate binding units, thus providing three possible binding site/binding site interacting pairs for each metal (Fig. 6a). Application of eqn (11) to equilibrium (7) thus transforms the original model (eqn (8)) into eqn (12).

$$\beta^{Ga,L4}_{2,3} = 1536(f^{Ga,L4}_{inter})^6(EM^{Ga,L4})^2(u^{Ga,Ga})(u^{L4,L4})^6 \quad (12)$$

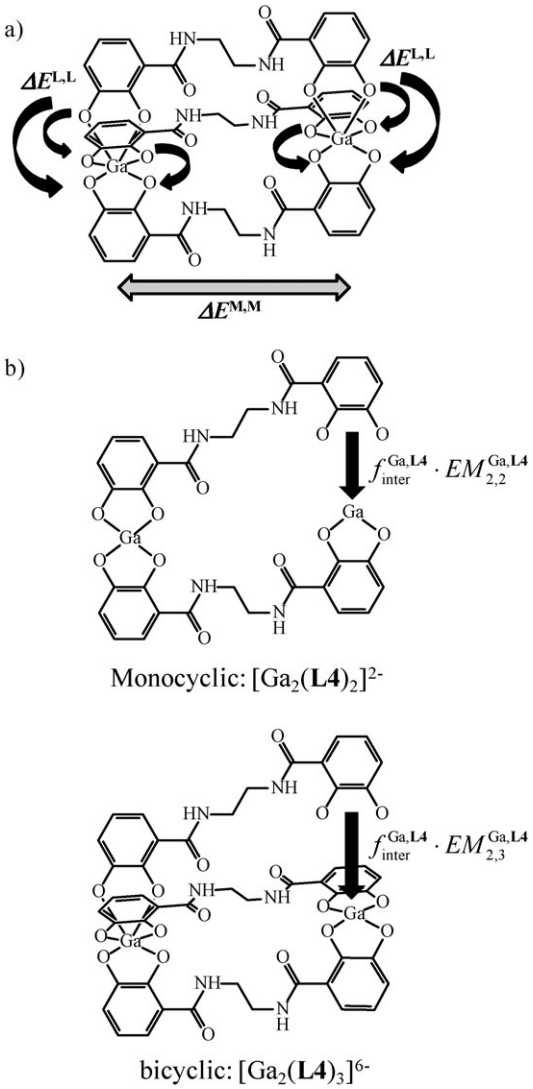

Fig. 6 Schematic illustrations and countings of (a) homo-component interactions and (b) intramolecular connections in the self-assembly of the triple-stranded helicate $[Ga_2(\mathbf{L4})_3]^{6-}$.

Since the formation of $[Ga_2(\mathbf{L4})_3]^{6-}$ requires two successive intramolecular connection, there is no obvious reason for which the effective molarity $EM^{Ga,L4}_{2,2}$ controlling the formation of the monocyclic intermediate $[Ga_2(H_2O)_4(\mathbf{L4})_2]^{2-}$ should be equal to $EM^{Ga,L4}_{2,3}$ transforming the latter complex into the final bicyclic helicate $[Ga_2(\mathbf{L4})_3]^{6-}$ (Fig. 6b). In other words, $EM^{Ga,L4}_{2,2} = EM^{Ga,L4}_{2,3} = EM^{Ga,L4}$ corresponds to a non-cooperative behaviour, while $EM^{Ga,L4}_{2,2} < EM^{Ga,L4}_{2,3}$ (respectively $EM^{Ga,L4}_{2,2} > EM^{Ga,L4}_{2,3}$) implies positive, (respectively negative) cooperativity. Eqn (12) should therefore be rewritten to give

$$\beta^{Ga,L4}_{2,3} = 1536(f^{Ga,L4}_{inter})^6(EM^{Ga,L4}_{2,2})(EM^{Ga,L4}_{2,3})(u^{Ga,Ga})(u^{L4,L4})^6 \quad (13)$$

We are now equipped for the experimental determination of the five parameters controlling the stability of the self-assembled triple-stranded helicate $[Ga_2(\mathbf{L4})_3]^{6-}$ according that a sufficient number of experimental stability constants (> 5) are accessible

for complexes of the same family (including thermodynamic intermediates or competitors).[18,22] For the reader exclusively interested in the application of the additive free energy model (eqn (11)) to practical metallo-supramolecular assemblies, please skip directly to section 6. The three next sections aim at unravelling and understanding the physical origins of the five thermodynamic microscopic describers involved in eqn (11), with the ultimate goal of providing structure–properties relationships compatible with the chemical programming of metallo-supramolecular assemblies.

3. A purely entropic driving force: the rotational statistical factor $\omega_{pm,pn}^{M,L}$

Intuitively, the estimation of the pure entropic driving force resulting from the change in rotational degeneracy accompanying the transformation of the reactants into products according to equilibrium (1) can be simply obtained by the ratio l/r, where l is the number of chemically plausible different sets (or microspecies) of $[M_{pm}L_{pn}]$ that can be formed if all the identical atoms of M and L are labelled, r corresponding to the same definition for the opposite reaction.[30]

$$pm\,M + pn\,L \underset{r}{\overset{l}{\rightleftharpoons}} [M_{pm}L_{pn}]\beta_{pm,pn}^{M,L} \qquad (1)$$

This procedure is straightforward when a limited number of hetero-component interactions are involved, as illustrated by the formation of the hydrogen bound array shown in Fig. 7.[21d] The bidentate hydrogen acceptor A possesses two identical nitrogen atoms, numbered N_1 and N_2, while each phenol donor D possesses a single hydrogen donor group numbered O1. Whatever the organization of the phenol groups, the formation of the two hetero-component connections leading to AD_2 produces the same microspecies and $l = 1$ (Fig. 7a). Moreover, there is always a single way, *i.e.* $r = 1$, in which the constituent building blocks of a self-assembly can be formed from an adduct exclusively obtained by addition reaction.[24]

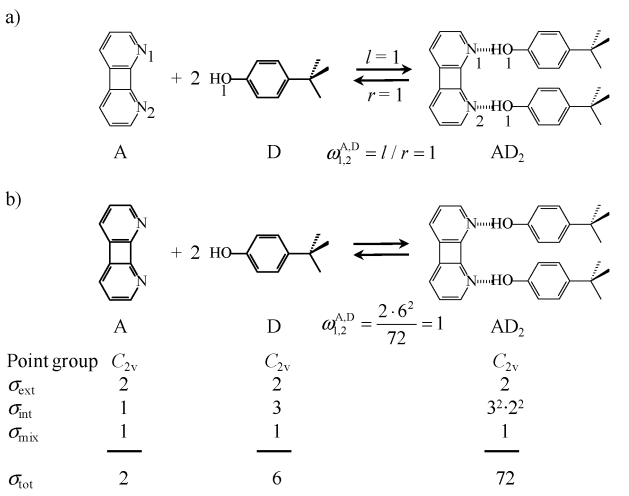

Fig. 7 Formation of the hydrogen bound $[AD_2]$ array[21d] and calculation of the intrinsic rotational statistical factor by using (a) the direct counting method[30] or (b) the symmetry number method.[31]

We obviously conclude that $\omega_{1,2}^{A,D} = l/r = 1$. The same result can be obtained by using the symmetry number method, which may appear tedious for this simple case (Fig. 7b). According to Benson,[31] the statistical factor $\omega_{1,2}^{A,D}$ is given by the ratio of the symmetry numbers for reactants and product species shown in eqn (6). The underlying concept is derived from the fact that the symmetry number of a molecule, σ, affects its rotational entropy by a factor $-R\ln(\sigma)$.[31] The factor σ is indeed the product of the external (σ_{ext}) and internal (σ_{int}) symmetry numbers, modulated by the mixing entropy produced by the number of isomeric microspecies contributing to the macrospecies (σ_{mix}).[24]

$$\sigma_{tot} = \sigma_{ext}\sigma_{int}\sigma_{mix} \qquad (14)$$

The external symmetry number is defined as the number of different, but indistinguishable atomic arrangements that can be obtained by rotating a given molecule as a whole. It is found in practice by multiplying the orders of the independent symmetry operations of the first kind (*i.e.* not involving inversion centre or symmetry plane) of the point group to which the molecule belongs (axes of infinite order are not considered because they do not generate different atomic arrangements). For the C_{2v} point group involved for all the partners leading to the hydrogen bound array AD_2 (Fig. 7b), a single independent twofold rotation axis has to be taken into account and $\sigma_{ext} = 2$ (Table 1).

The internal symmetry number is similarly defined, but for internal rotations about single bonds. For the phenol donor component D, the *tert*-butyl substituent is located onto a threefold internal rotation axis and $\sigma_{int}(D) = 3$ (Fig. 7b). In the final complex AD_2, we find two internal threefold rotation axes associated with the two *tert*-butyl group of the bound D components, and two internal twofold rotation axes passing through the N–HO bonds, thus leading to $\sigma_{int}(AD_2) = 3^2 \cdot 2^2 = 36$. Finally, a correction for the mixing entropy, σ_{mix}, produced by the existence of chemically distinguishable isomeric species at equilibrium, must be systematically estimated.[24] Its mathematical derivation is beyond the scope of this feature article and can be found in ref. 24, but we note that the entropy of mixing reduces the apparent symmetry number to $\sigma_{app} = \sigma/x$ when one considers a mixture containing x isomeric species, and thus $\sigma_{mix} = 1/x$.[24] The only common use of this correcting factor for metallo-supramolecular self-assemblies concerns chiral molecules or complexes, which exist as racemic mixtures of their enantiomers. In the latter case $x = 2$, and we introduce $\sigma_{mix} = 1/x = 1/2$ to account for the

Table 1 External symmetry numbers for various point groups[24]

Point group	σ_{ext}
C_1, C_i, C_s, $C_{\infty v}$, R_3	1
$D_{\infty h}$	2
C_n, C_{nv}, C_{nh}	n
D_n, D_{nd}, D_{nh}	$2n$
S_n (n even)	$n/2$
T_d	12
O_h	24
I_h	60

entropy of mixing. Since A, D and AD_2 shown in Fig. 7b belong to the achiral C_{2v} point group, $x = 1$ and $\sigma_{mix} = 1$. From the total symmetry numbers, σ_{tot} (Fig. 7b), we eventually calculate $\omega_{1,2}^{A,D} = (2{\cdot}6^2)/72 = 1$ by using eqn (6).

The power of the symmetry number method becomes evident with more complicated assemblies, such as the formation of the triple-stranded helicate $[Ga_2(\mathbf{L4})_3]^{6-}$ (equilibrium (7), Fig. 8). Once the point groups of all the partners involved in the self-assembly are at hand, it is trivial to calculate the external symmetry numbers by using Table 1. The internal symmetry numbers are limited to the internal rotations of the water molecules about their two fold axis in $[Ga(H_2O)_6]^{3+}$ and a correction for the mixing entropy comes from the formation of the D_3-symmetrical triple-stranded helicate, which is the only chiral partner existing as a pair of enantiomers in the assembly process (Fig. 8a). The application of eqn (6) eventually gives $\omega_{2,3}^{Ga,\mathbf{L4}} = 1536$ (Fig. 8a).

The application of the direct counting method to equilibrium (7) benefits from the fact that only $[Ga_2(\mathbf{L4})_3]^{6-}$ possesses different contributing microspecies when all identical connecting atoms are labelled (Fig. 8b). In other words, $r = 1$ and l corresponds to the degeneracy of $[Ga_2(\mathbf{L4})_3]^{6-}$, which can be considered as made up by two octahedral metals, each presenting a trigonal face for its connection to its homologue *via* three linear linkers (Fig. 8b). Since each octahedron possesses eight different trigonal faces, there are $8 \times 8 = 64$ possibilities for arranging the pairs of labelled octahedral metals in the binuclear complex. Once a pair of trigonal face is selected, there are three more possibilities for matching the three different labels borne by each face, thus leading to $64 \times 3 = 192$ possibilities. If we now introduce the four possible arrangements of the three ligand strands corresponding to head-to-head-to-head (one possibility) and head-to-head-to-tail (three possibilities) organizations, we obtain $192{\times}4 = 768$ microspecies for each enantiomer of $[Ga_2(\mathbf{L4})_3]^{6-}$, which can be formed by the various combinations of the reactants. Finally, the self-assembly process being not enantioselective, both enantiomers are obtained in a racemic mixture thus giving $l = 2 \times 768 = 1536$ and $\omega_{2,3}^{Ga,\mathbf{L4}} = l/r = 1536/1 = 1536$. Although both methods obviously provide

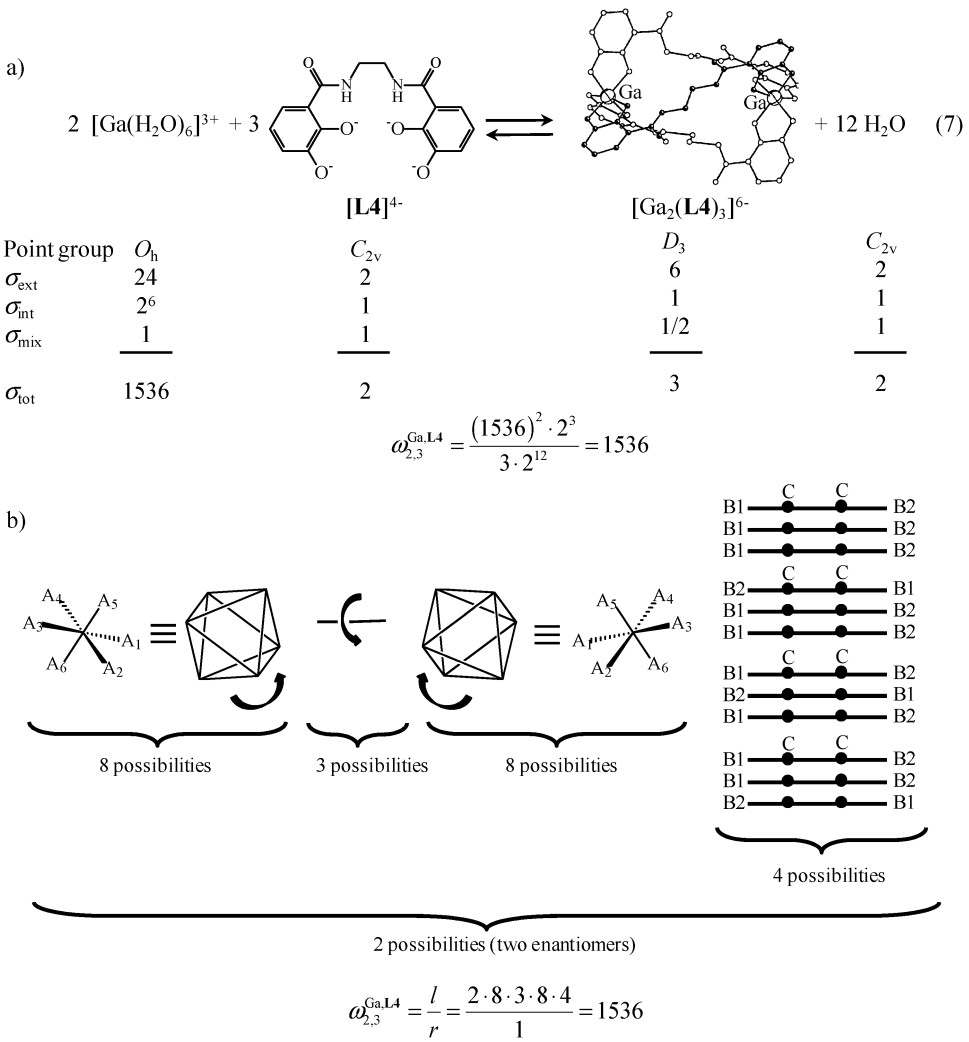

Fig. 8 Calculation of the rotational statistical factor for equilibrium (7) by using (a) the symmetry number method and (b) the direct counting method.

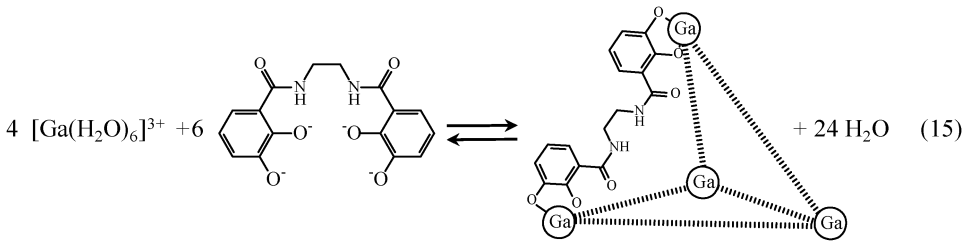

Point group	O_h	C_{2v}	T	C_{2v}
σ_{ext}	24	2	12	2
σ_{int}	2^6	1	1	1
σ_{mix}	1	1	1/2	1
σ_{tot}	1536	2	6	2

$$\omega_{2,3}^{Ga,L4} = \frac{(1536)^4 \cdot 2^6}{6 \cdot 2^{24}} = 3538944$$

Fig. 9 Calculation of the rotational statistical factor for equilibrium (15) by using the symmetry number method.

identical statistical factors, the intellectual efforts are much reduced by using the symmetry number method, as illustrated by the straightforward calculation of $\omega_{4,6}^{Ga,L4} = 3538944$ for the formation of the tetrahedral cage $[Ga_4(\mathbf{L4})_6]^{12-}$ (equilibrium (15), Fig. 9).

$$4\,[Ga(H_2O)_6]^{3+} + 6\,[\mathbf{L4}]^{4-} \rightleftharpoons [Ga_4(\mathbf{L4})_6]^{12-} + 24\,H_2O;\ \beta_{4,6}^{Ga,L4} \quad (15)$$

Interestingly, the combination of equilibria (7) and (15) corresponds to the simple dimerization reaction

$$2\,[Ga_2(\mathbf{L4})_3]^{6-} \rightleftharpoons [Ga_4(\mathbf{L4})_6]^{12-};\ \beta_{dim}^{Ga,L4} \quad (16)$$

for which $\beta_{dim}^{Ga,L4} = \beta_{4,6}^{Ga,L4}/(\beta_{2,3}^{Ga,L4})^2$ and thus $\omega_{dim}^{Ga,L4} = \omega_{4,6}^{Ga,L4}/(\omega_{2,3}^{Ga,L4})^2 = 3/2$. In other words, the contribution of the rotational degeneracy to the dimerization process favors the formation of the supramolecular object containing the larger number of components by $\Delta g_{dim}^{stat} = -RT\ln(\omega_{dim}^{Ga,L4}) = -1.0$ kJ mol^{-1}. Though limited in magnitude, it is worth stressing here that this statistical contribution is opposed to the classical entropic arguments solely based on the changes in translational entropies, which should systematically penalize the formation of a dimer over two monomers.

4. The hetero-component connections as the prime thermodynamic effects: $f_{inter}^{M,L}$ and $f_{intra}^{M,L}$

The intermolecular hetero-component connection, modeled with the microscopic parameter $f_{inter}^{M,L}$, corresponds to the standard complexation process during which a set of solvent molecules bound to the metal are replaced by the donor atoms of the ligand. This is easily illustrated with the formation of the 1 : 1 nitrato lanthanide complexes $[Ln(\mathbf{L}k)(NO_3)_3]$, whereby three acetonitrile molecules are expelled by the entering tridentate ligand (k = 5–7, equilibrium (17) and Fig. 10). The stability constants modeled with eqn (11) indeed only resort to a specific statistical factor combined with the absolute affinity for intermolecular metal–ligand connection (eqn (18) and Fig. 10).

$$[Ln(NO_3)_3(CH_3CN)_3] + \mathbf{L}k \rightleftharpoons [Ln(NO_3)_3(\mathbf{L}k)] + 3\,CH_3CN;\ \beta_{1,1}^{Ln,Lk} \quad (17)$$

$$\beta_{1,1}^{Ln,Lk} = \omega_{1,1}^{Ln,Lk} f_{inter}^{Ln,Lk} \quad (18)$$

Once the statistical factors have been calculated by using the symmetry number method (Fig. 10), the application of eqn (18) for analyzing the experimental stability constants collected into Table 2 (column 3) leads to the free energy changes $\Delta g_{inter}^{Ln,Lk} = -RT\ln(f_{inter}^{Ln,Lk})$ accompanying the replacement of three acetonitrile molecules[32] by the tridentate N_3 or N_2O binding sites of ligand $\mathbf{L}k$ (Table 2, column 5).[33,34]

We first notice that the N_3 binding site found in **L5** is as efficient as the N_2O sites found in **L6** and **L7**, despite the well-known ukase of coordination chemistry, which states that trivalent lanthanides are mainly oxophilic. We also note that the peripheral substitution of the benzimidazole ring on going from **L6** to **L7** slightly decreases $f_{inter}^{Ln,Lk}$, while a considerable increase of the latter parameter is observed along the lanthanide series for a given ligand ($f_{inter}^{La,Lk} \leq f_{inter}^{Eu,Lk} \ll f_{inter}^{Lu,Lk}$), in line with the classical electrostatic model developed by Choppin for lanthanide complexation.[35] Since $\Delta g_{inter}^{Ln,Lk}$ corresponds to a balance between intermolecular bond breaking (release of solvent molecules) and bond making (fixation of the entering ligand), it obviously depends on the solvent, on the counter-anions and on the ionic strength. For instance, the formation of $[Ln(\mathbf{L5})(CF_3SO_3)_3]$ in acetonitrile, whereby nitrate counter-anions are replaced with trifluoromethane sulfonates, gives $-42 \leq \Delta g_{inter}^{Ln,L5}(CF_3SO_3) \leq -34$ kJ mol^{-1},[33] a free energy change approximately 10 kJ mol^{-1} more favourable than that found for $[Ln(\mathbf{L5})(NO_3)_3]$ (Table 2). The addition of NBu_4ClO_4 (0.01 M in acetonitrile) as an inert electrolyte for fixing the ionic strength, further favors $\Delta g_{inter}^{Ln,L5}(CF_3SO_3)$ by an additional 10 kJ mol^{-1} bonus.[36]

According to eqn (9), the replacement of an intermolecular connection process, $f_{inter}^{M,L}$, with its intramolecular counter-part

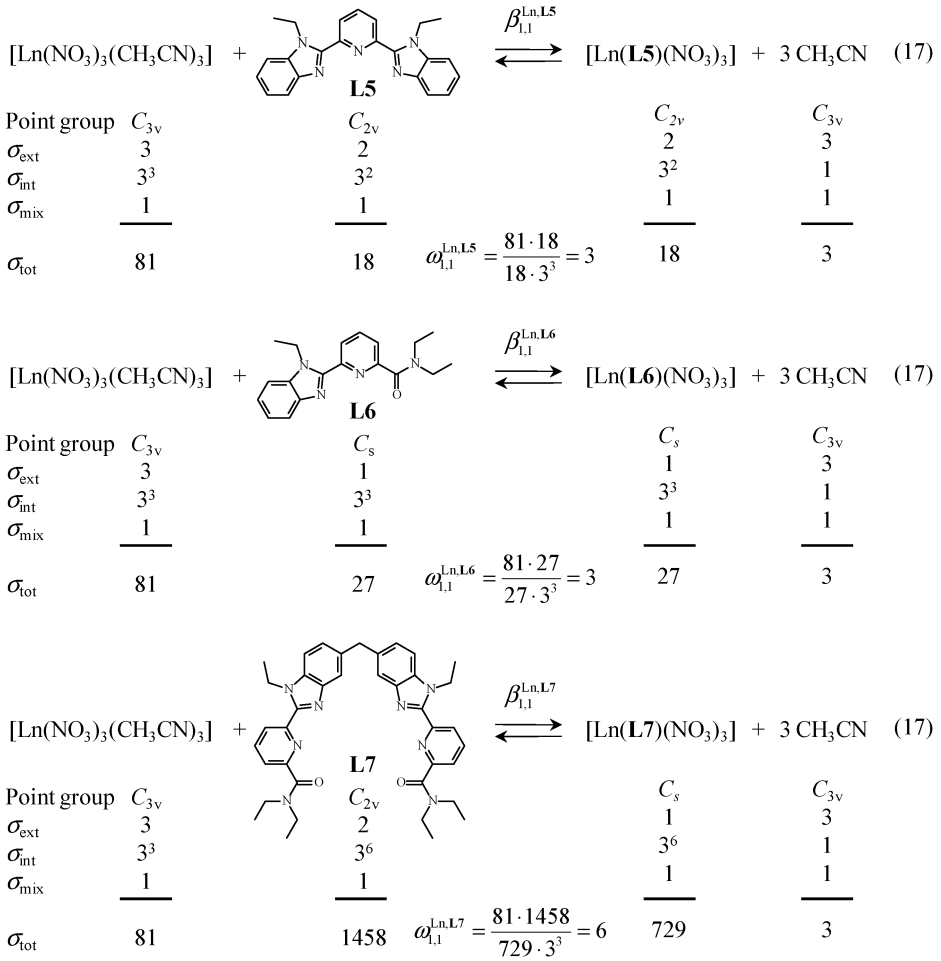

Fig. 10 Computed symmetry numbers (σ) and statistical factors ($\omega_{1,1}^{Ln,Lk}$) for the complexation of nine-coordinate $[Ln(NO_3)_3(CH_3CN)_3]$ to **L5**–**L7** in acetonitrile. The somewhat arbitrary choice[32] of an ideal C_{3v} symmetry for the metallic unit $[Ln(NO_3)_3(CH_3CN)_3]$ is not crucial since each equilibrium refers to the same starting metal-containing entity.

Table 2 Selected thermodynamic formation constants for $[Ln(NO_3)_3(\mathbf{L}k)]$ (k = 5–7, Ln = La, Eu, Lu, acetonitrile, 298 K)[33,34]

Ligand	Ln^{III}	$\log(\beta_{1,1}^{Ln,Lk})$	$\omega_{1,1}^{Ln,Lk}$	$\Delta g_{inter}^{Ln,Lk}$ /kJ mol^{-1}
L5	La	4.98(8)	3	−25.7(5)
L5	Eu	4.71(5)	3	−24.1(3)
L5	Lu	6.40(9)	3	−33.8(5)
L6	La	5.27(6)	3	−27.3(3)
L6	Eu	5.27(9)	3	−27.3(5)
L6	Lu	6.06(9)	3	−31.8(5)
L7	La	5.09(9)	6	−24.6(5)
L7	Eu	5.49(4)	6	−26.9(3)
L7	Lu	5.79(9)	6	−28.6(5)

$f_{intra}^{M,L} = f_{inter}^{M,L}EM$ simply requires a multiplication by the correcting EM factor, which takes into account the difference in enthalpic and entropic contributions for these two processes. In absence of ring strain ($\Delta H_{intra}^{M,L} = \Delta H_{inter}^{M,L}$), and for a freely jointed chain composed of a large number of linkers, the effective molarity EM can be approached by a statistical theory, which neglects excluded volume effects.[27] In these conditions, EM can be considered as a measure of the probability of the two terminal binding units of the ligand strand to fix the same metal (Fig. 11a). Assuming a statistical Gaussian exploration of space, the probability density $W(x,y,z)$, expressed in molecule per dm^3, of finding one end (x,y,z) at a distance r from the other end located at the origin (0,0,0), can be evaluated with eqn (19), whereby β depends on the chain length *via* its mean square end-to-end distance $\langle r^2\rangle$ given in eqn (20).[27]

$$W(x,y,z) = \left(\frac{\beta}{\pi^{1/2}}\right)^3 \exp(-\beta^2 r^2) \qquad (19)$$

$$\beta = \left(\frac{3}{2\langle r^2\rangle}\right)^{1/2} \qquad (20)$$

For an intramolecular connection process involving the complexation of the two binding sites of the ligand strand to the same metal located at the origin $\langle 0,0,0\rangle$, r tends to zero (Fig. 11a) and the combination of eqn (19) and (20) gives eqn (21) whereby $W(0,0,0)/N_{Av}$ is the target effective molarity expressed in mole per dm^3.[37]

$$EM(r=0) = \frac{W(0,0,0)}{N_{Av}} = \frac{1}{N_{Av}}\left(\frac{\beta}{\pi^{1/2}}\right)^3 = \frac{1}{N_{Av}}\left(\frac{3}{2\pi\langle r^2\rangle}\right)^{3/2} \qquad (21)$$

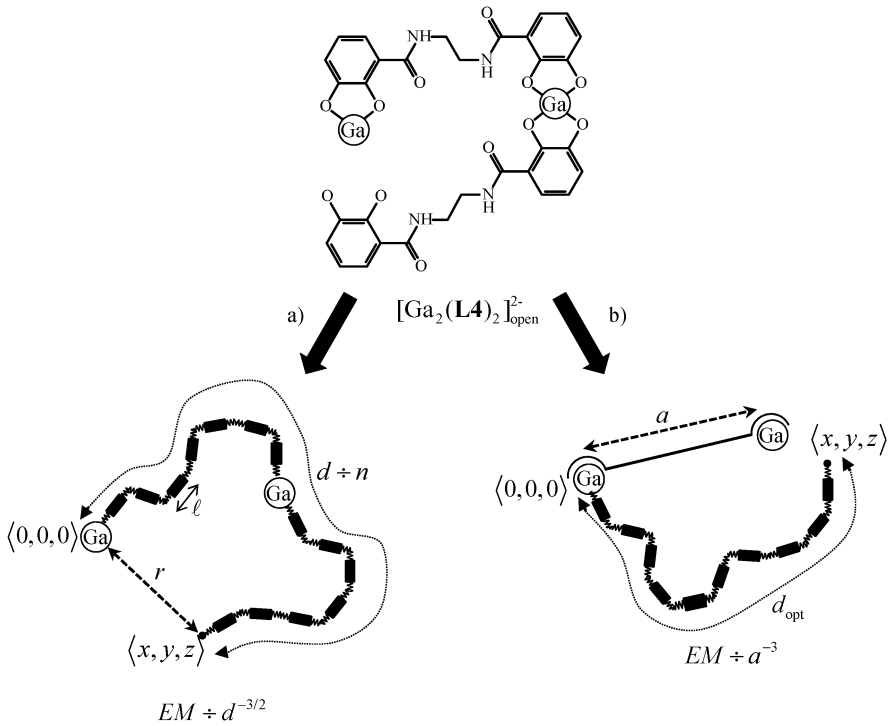

Fig. 11 A rough modeling of the effective molarity for the macrocyclization process operating in $[Ga_2(\mathbf{L4})_2]^{2-}_{open}$ by using Kuhn's theory:[27] (a) the two ligand strands connected by the intermediate metal are considered as a freely jointed chain, and (b) the second ligand is considered as a freely jointed chain with an optimized length for the connection of two metals held at a distance a.

For a freely jointed chain, *i.e.* a long and highly flexible chain made up of n small segments of length l, the mean square end-to-end distance is given by $\langle r^2 \rangle = nl^2$.[27] Substitution into eqn (21) eventually shows that $EM(r = 0) \div n^{-3/2}$, and since the number of segments n is itself proportional to the total length of the chain d, we can write $EM(r = 0) \div d^{-3/2}$ (Fig. 11a).[27,38] For a real chain, $\langle r^2 \rangle = C_n nl^2$, where $C_n > 1$ is an empirical factor which takes into account the fact that real chains are more stiff than freely jointed chains. C_n also depends on n, but reach a constant value C_∞ for large values of n. The resulting $EM(r = 0) \div d^{-3/2}$ dependence on chain length for flexible ligands contrasts with the widespread opinion that $EM(r = 0) \div d^{-3}$, which is erroneously deduced from the intuition that the end of the chain has to explore some volume elements prior to perform the intramolecular connection.[8c,e]

This confusion probably results from the consideration of a closely related problem in metallo-supramolecular chemistry, in which two metals are held at a fixed distance a by a rigid spacer, while a bivalent ligand is responsible for the macrocyclization process (Fig. 11b). After intermolecular binding of one extremity of the ligand strand to metal 1, the second connection process involving metal 2 is intramolecular, and its effective molarity is simply given by introducing $r = a$ into eqn (19) to give eqn (22).

$$EM(r = a) = \frac{W(r = a)}{N_{Av}} = \frac{1}{N_{Av}} \left(\frac{\beta}{\pi^{1/2}} \right)^3 \exp(-\beta^2 a^2) \quad (22)$$

Since β depends on the length of the ligand strand (eqn (20)), $EM(r = a)$ will go through a maximum for an optimized length d_{opt} of the flexible ligand. This problem was originally solved by using a trial/error procedure,[27j] but Ercolani proposed an elegant solution with the simple differentiation of eqn (22) with respect to β in order to give eqn (23), which is finally equated to zero.[38]

$$\frac{dEM(r = a)}{d\beta} = \frac{\beta^2}{N_{Av}\pi^{3/2}} (3 - 2\beta^2 a^2) \exp(-\beta^2 a^2) = 0 \quad (23)$$

Solving eqn (23) gives $\beta = (3/2)^{1/2} a^{-1}$, which can be introduced into eqn (22) to give eqn (24).

$$EM(r = a)_{max} = \frac{1}{N_{Av} a^3} \left(\frac{3}{2\pi} \right)^{3/2} \exp(-3/2) \quad (24)$$

We now obtain the well-accepted $EM \div a^{-3}$ dependence, in which a is the separation between the two binding sites, but this behaviour is only valid for a long and flexible chain of optimized length d_{opt} (Fig. 11b). Altogether, the above-mentioned Kuhn theory[27] could be helpful for roughly estimating the dependence of the entropic part of EM (i) with respect to the distance d separating the termini of the binding sites in a simple ligand strand (chelate effect, $EM \div d^{-3/2}$ Fig. 11a), or (ii) with respect to the gap a separating two coordination sites connected by a bidentate chelating ligand possessing an optimized length (preorganization, $EM \div a^{-3}$ Fig. 11b). Obviously, real cases should incorporate enthalpic ring strains as a major contribution, and EM merely corresponds to an experimental factor correlating the inter- and intramolecular absolute affinities of the metal for a given binding site ($f^{M,L}_{intra} = f^{M,L}_{inter} EM$). However, if we assume that the ring strains affecting two closely related intramolecular processes are comparable, the

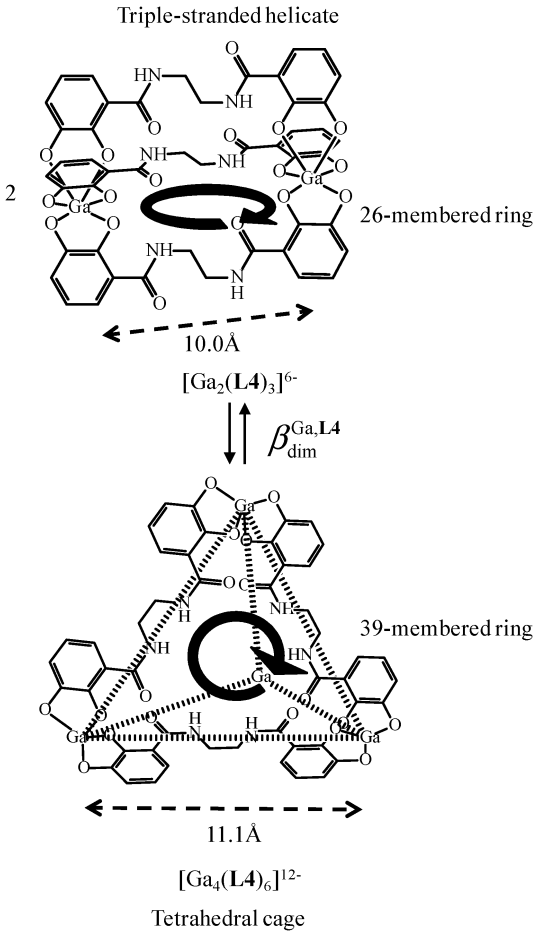

Fig. 12 Schematic representation of the dimerization process described in equilibrium (16) highlighting the intramolecular connection processes. The separation between the binding sites are taken from the crystal structures of the isolated complexes.[23]

use of eqn (21) and (24) may limit the number of microscopic parameters required for modeling the possible output of a self-assembly process (see section 6). This approach can be illustrated with our working example, in which two triple-stranded helicates $[Ga_2(\mathbf{L4})_3]^{6-}$ dimerize to give the tetrahedral cage $[Ga_4(\mathbf{L4})_6]^{12-}$ (equilibrium (16), Fig. 12).

Neglecting any homo-component interactions ($\Delta E^{Ga,Ga} = 0$ and $\Delta E^{\mathbf{L4},\mathbf{L4}} = 0$, their explicit consideration as perturbation are discussed in the next section), the application of eqn (11) for equilibria (7) and (15) leads to (the statistical factors are calculated in Fig. 8 and 9)

$$\beta_{2,3}^{Ga,\mathbf{L4}} = 1536(f_{inter}^{Ga,\mathbf{L4}})^6(EM_{2,3}^{Ga,\mathbf{L4}})^2 \quad (25)$$

$$\beta_{4,6}^{Ga,\mathbf{L4}} = 3528944(f_{inter}^{Ga,\mathbf{L4}})^{12}(EM_{4,6}^{Ga,\mathbf{L4}})^3 \quad (26)$$

Since (i) $\beta_{dim}^{Ga,\mathbf{L4}} = \beta_{4,6}^{Ga,\mathbf{L4}}/(\beta_{2,3}^{Ga,\mathbf{L4}})^2$ and (ii) $f_{inter}^{Ga,\mathbf{L4}}$ can be reasonably assumed to be similar for the connection of a Ga^{III} cation to the bidentate catecholate unit in both complexes, we obtain

$$\beta_{dim}^{Ga,\mathbf{L4}} = \frac{3}{2}\frac{(EM_{4,6}^{Ga,\mathbf{L4}})^3}{(EM_{2,3}^{Ga,\mathbf{L4}})^4} \quad (27)$$

The first 3/2 term results from the ratio of the statistical (rotational) factors and it has been already discussed (see previous section). The second ratio can be estimated if we assume that (i) the steric constraints accompanying the intramolecular macrocyclization processes are similar in the two closely related complexes $[Ga_2(\mathbf{L4})_3]^{6-}$ and $[Ga_4(\mathbf{L4})_6]^{12-}$ and (ii) the ligand strands possess optimal lengths and flexibility for connecting two Ga^{III} rigidly held at $a_{2,3}^{Ga,\mathbf{L4}} = 10.0$ Å in $[Ga_2(\mathbf{L4})_3]^{6-}$, and at $a_{4,6}^{Ga,\mathbf{L4}} = 11.1$ Å in $[Ga_4(\mathbf{L4})_6]^{12-}$ (Fig. 12).[23] In these conditions, eqn (24) implies that $EM_{4,6}^{Ga,\mathbf{L4}}/EM_{2,3}^{Ga,\mathbf{L4}} = (a_{2,3}^{Ga,\mathbf{L4}}/a_{4,6}^{Ga,\mathbf{L4}})^3 = (10.0/11.1)^3 = 0.73$. Introducing this ratio into eqn (27) eventually leads to

$$\beta_{dim}^{Ga,\mathbf{L4}} = \frac{3}{2}(0.73)^3\frac{1}{EM_{2,3}^{Ga,\mathbf{L4}}} = \frac{0.58}{EM_{2,3}^{Ga,\mathbf{L4}}} \quad (28)$$

Obviously, the numerator in eqn (28) drastically depends on the specific ring strains accompanying the macrocyclization of 26-membered rings in $[Ga_2(\mathbf{L4})_3]^{6-}$ and 39-membered rings in $[Ga_4(\mathbf{L4})_6]^{12-}$ (Fig. 12). We therefore re-write eqn (28) under the general form $\beta_{dim}^{Ga,\mathbf{L4}} = \alpha/EM_{2,3}^{Ga,\mathbf{L4}}$, which highlights some interesting trends for the dimerization reaction. Firstly, the statistical factor favors the formation of the tetranuclear cage because of the relaxation of the rotational degeneracy. Secondly, any reduction in enthalpic ring strain in going from $EM_{2,3}^{Ga,\mathbf{L4}}$ (26-membered metallomacrocycle, Fig. 12 top) to $EM_{4,6}^{Ga,\mathbf{L4}}$ (39-membered metallomacrocycle, Fig. 12 bottom) increases α, and thus also favors the formation of the tetranuclear cage. Finally, the replacement of four intramolecular bonds in the reactants (*i.e.* two macrobicyclic triple-stranded helicates) with only three intramolecular connections in the product (*i.e.* a single macrotricyclic cage) is responsible for the denominator of eqn (28). The better the preorganization for macrocyclization ($EM_{2,3}^{Ga,\mathbf{L4}}$ is large), the smaller $\beta_{dim}^{Ga,\mathbf{L4}}$ is, and the classical inference solely based on translational entropy holds. Formally speaking, when $EM_{2,3}^{Ga,\mathbf{L4}} \geq \alpha(C_{tot}/3)$, then $\beta_{dim}^{Ga,\mathbf{L4}} \leq (3/C_{tot})$ and the tetranuclear dimeric cage represents less than 50% of the ligand speciation in solution at equilibrium ($C_{tot} = 3|[Ga_2(\mathbf{L4})_3]^{6-}| + 6|[Ga_4(\mathbf{L4})_6]^{12-}|$ is the total concentration of ligand). In other words, the magnitude of the effective molarity is crucial for the selection of one specific complex among a library of systems possessing variable numbers of metallo-macrocycles. The above $2\ [Ga_2(\mathbf{L4})_3]^{6-} \leftrightarrow [Ga_4(\mathbf{L4})_6]^{12-}$ working example (eqn (16)) suggests that the (deliberate) design of unfavorable macrocyclization processes (small values of *EM*) due to severe ring strains and/or poor preorganization indeed favors the formation of polynuclear complexes including a maximum of components with a minimum of macrocycles. The recent and remarkable observations reported by Ward and co-workers[14q,14t] on the recurrent 'magical' preferences for the formation of complicated d-block or f-block polynuclear clusters, instead of the planned binuclear multiple-stranded helicates, probably find their origin in the very small magnitudes of the effective molarities resulting from the introduction of rigid aromatic spacers which maximize ring strains (Fig. 3). According to a quantitative point of view, eqn (28) is very attractive for the experimental determination of *EM*, because it only requires the determination of the dimerization constant $\beta_{dim}^{Ga,\mathbf{L4}}$. However, the rough

a) Chemical structures

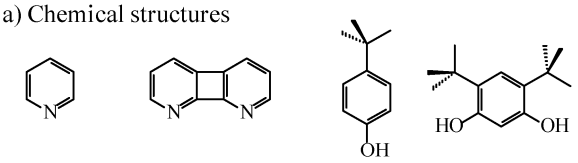

A AA D DD

b) Thermodynamic equilibria

$$A + D \rightleftharpoons A{\bullet}D \quad \beta_{1,1}^{A,D} \quad (29)$$

$$AA + 2\,D \rightleftharpoons AA{\bullet}D_2 \quad \beta_{1,2}^{AA,D} \quad (30)$$

$$2\,A + DD \rightleftharpoons DD{\bullet}A_2 \quad \beta_{2,1}^{A,DD} \quad (31)$$

$$AA + DD \rightleftharpoons DD{\bullet}AA \quad \beta_{1,1}^{AA,DD} \quad (32)$$

c) Thermodynamic modeling

$$\beta_{1,1}^{A,D} = f_{inter}^{A,D} \quad (33)$$

$$\beta_{1,2}^{AA,D} = \left(f_{inter}^{A,D}\right)^2 \left(u^{A,A}\right)^2 \quad (34)$$

$$\beta_{2,1}^{A,DD} = \left(f_{inter}^{A,D}\right)^2 \left(u^{D,D}\right)^2 \quad (35)$$

$$\beta_{1,1}^{AA,DD} = 2\left(f_{inter}^{A,D}\right)^2 \left(u^{A,A}\right)^2 \left(u^{D,D}\right)^2 EM \quad (36)$$

Fig. 13 Chemical double mutant cycle for quantifying the energy benefit ($-RT\ln(EM)$) associated with the intranuclearity of the second H-bond in the AA·DD complex.[21c]

assumptions leading to the numerator in eqn (28) prevents a direct and reliable estimation of *EM* with this technique. Nevertheless, the underlying idea of comparing closely related systems differing by a single intramolecular process has been exploited by Hunter and co-workers in chemical double mutant cycle (equilibria (29)–(32), Fig. 13).[21d] The thermodynamic modeling of equilibria (29)–(32) with the site binding model (eqn (11)) requires two homo-component corrections $u^{A,A}$ and $u^{D,D}$, which adapt the free energy of each intermolecular hydrogen bonding when the two acceptors (in AA) or the two donors (in DD) are incorporated in a single molecule. A judicious combinations of eqn (33)–(36) gives

$$\frac{\beta_{1,1}^{AA,DD}(\beta_{1,1}^{A,D})^2}{\beta_{1,2}^{AA,D}\beta_{2,1}^{A,DD}} = 2EM \quad (37)$$

which allows the reliable determination of *EM* from the simple determination of the four association constants shown in Fig. 13.[21d] Depending on the solvent (CCl_4, $CHCl_3$, cyclohexane, 1,2-dichloroethane), Hunter and co-workers found $3 \leq EM \leq 33$ M, which indicates a very efficient preorganization of the rigid AA and DD building blocks for performing the intramolecular hydrogen bond leading to the monocyclic AA•DD complex.

Closely related strategies have been followed for estimating *EM* for the assembly of metal-mediated assemblies of porphyrins,[39] but we are not aware of similar simple estimation of *EM* in the field of multi-component polynuclear complexes.

5. The homo-component interactions as perturbations: $\Delta E^{L,L}$ and $\Delta E^{M,M}$

Once the complex $[M_{pm}L_{pn}]$ has been assembled by using some favorable hetero-component connections resulting from a good match between the ligand binding possibilities and the stereochemical preferences of the metal ions, its stability is further modulated by the operation of the homo-component interactions (M···M and **L**···**L**), which thus contribute to the deviation from statistical binding (*i.e.* cooperativity). The stepwise replacement of water molecules with ammonia ligands around Ni(II) (equilibrium (38)) is a well-documented system, for which the successive stability constants (K_{n+1}^{Ni,NH_3} in eqn (39)) cannot be rationalized without considering some repulsive interligand interactions ($u^{NH_3,NH_3} = \exp(-\Delta E^{NH_3,NH_3}/RT) < 1$).[18b]

$$[Ni(H_2O)_n(NH_3)_{6-n}]^{2+} + NH_3 \rightleftharpoons [Ni(H_2O)_{n-1}(NH_3)_{6-n+1}]^{2+} + H_2O;\ K_{n+1}^{Ni,NH3} \quad (38)$$

$$K_{n+1}^{Ni,NH_3} = \frac{C_{n+1}^6}{C_n^6} f_{inter}^{Ni,NH_3} (u^{NH_3,NH_3})^n = \frac{(6-n)}{(n+1)} f_{inter}^{Ni,NH_3} (e^{-(\Delta E^{NH_3,NH_3}/RT)})^n \quad (39)$$

The multi-linear least-square fit of the six available successive stability constants (K_1^{Ni,NH_3} to K_6^{Ni,NH_3}) with two fitted parameters (f_{inter}^{Ni,NH_3} and u^{NH_3,NH_3}), indeed gives $\Delta g_{inter}^{Ni,NH_3} = -RT\ln(f_{inter}^{Ni,NH_3}) = -11.7$ kJ mol^{-1} for the balance between the desolvation of the metal and the formation of the intermolecular metal–nitrogen bond, and $\Delta E^{NH_3,NH_3} = 1.34$ kJ mol^{-1} for the anti-cooperative free energy correction brought by the fixation of two NH_3 ligands onto the same Ni(II) centre.[18b] At first sight, the minute magnitude of the homo-component interaction has been tentatively assigned to the limited steric bulk and neutral charge of the entering ammonia ligand. With this interpretation in mind, it is interesting to perform the same trivial thermodynamic analysis of the successive complexation of dipicolinate dianions $[\mathbf{L8}]^{-2}$ to trivalent lanthanides, Ln^{III}, along the 4f series (equilibrium (40), Fig. 14a).[40]

$$[Ln(H_2O)_9]^{3+} + n\,[\mathbf{L8}]^{2-} \rightleftharpoons [Ln(\mathbf{L8})_n(H_2O)_{9-3n}]^{(3-2n)+} + 3n\ H_2O\ \beta_{1,n}^{Ln,\mathbf{L8}} \quad (40)$$

Application of the site binding model (eqn (11)), gives eqn (41)–(43) for the three cumulative constants, in which the interligand pair interaction $u^{\mathbf{L8},\mathbf{L8}} = \exp(-\Delta E^{\mathbf{L8},\mathbf{L8}}/RT)$ is restricted to operate in the coordination sphere of the metal, and thus contributes once in $[Ln(\mathbf{L8})_2(H_2O)_3]^-$ (eqn (42)) and thrice in $[Ln(\mathbf{L8})_3]^{3-}$ (eqn (43)).[41]

$$\beta_{1,1}^{Ln,\mathbf{L8}} = 6 f_{inter}^{Ln,\mathbf{L8}} \quad (41)$$

$$\beta_{1,2}^{Ln,\mathbf{L8}} = 12 (f_{inter}^{Ln,\mathbf{L8}})^2 u^{\mathbf{L8},\mathbf{L8}} \quad (42)$$

$$\beta_{1,3}^{Ln,\mathbf{L8}} = 16 (f_{inter}^{Ln,\mathbf{L8}})^3 (u^{\mathbf{L8},\mathbf{L8}})^3 \quad (43)$$

For each lanthanide, the multi-linear least-square fit of eqn (41)–(43) to the experimental formation constants (Fig. 14b)[40] gives $\Delta g_{inter}^{Ln,\mathbf{L8}} = -RT\ln(f_{inter}^{Ln,\mathbf{L8}})$ (Fig. 14c) and $\Delta E^{\mathbf{L8},\mathbf{L8}}$ (Fig. 14d). In line with the electrostatic model developed

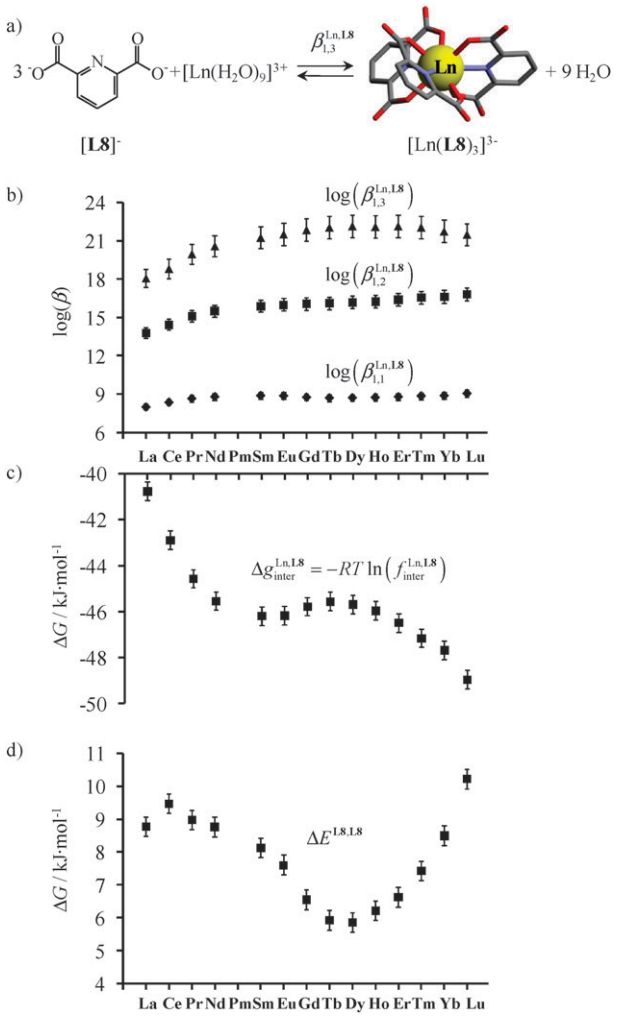

Fig. 14 (a) Schematic formation of the triple-stranded helical complex $[Ln(\mathbf{L8})_3]^{3-}$, (b) cumulative formation constants determined at 293 K in water (I = 0.5 M, $NaClO_4$),[40] (c) $\Delta g_{inter}^{Ln,L8} = -RT\ln(f_{inter}^{Ln,L8})$ and (d) $\Delta E^{L8,L8}$ fitted with eqn (41)–(43).

by *Choppin*,[35] the balance between the desolvation process and the formation of the metal–ligand bond gives more negative values for $\Delta g_{inter}^{Ln,L8}$ along the lanthanide series (Fig. 14c). All pair interligand interactions are repulsive and of the same magnitude ($5 \leq \Delta E^{L8,L8} \leq 11$ kJ mol^{-1}, Fig. 14d). If the origin of the wavy distribution of $\Delta E^{L8,L8}$ along the lanthanide series is beyond the scope of this tutorial review, the overall minute magnitude of $\Delta E^{L8,L8}$ for the pair interaction of two negatively charged ligands held at short distance raises some licit questioning about its physical origin, and its chemical tuning. Since charge delocalization over the entire ligand is a severe handicap for obtaining simple analytical formulation for homo-component interactions, we will approach this problem with the discussion of the closely related intermetallic pair interactions $\Delta E^{M,M}$. Let's consider the transfer of a spherical Lu^{3+} cation from the triple-stranded helicate $[RuLu(\mathbf{L9})_3]^{5+}$ into the trigonal $[Cr(\mathbf{L9})_3]^{3+}$ receptor to give $[CrLu(\mathbf{L9})_3]^{6+}$ and $[Ru(\mathbf{L9})_3]^{2+}$ (equilibrium (44) in Fig. 15).

If one reasonably assumes that the chemical affinity of the C_3-symmetrical nine-coordinating N_6O_3 binding site for Lu^{3+} is identical in the two binuclear helicates, the application of the site binding model (eqn (11)) in the gas phase implies that the free energy change accompanying the exchange reaction is simply given by

$$\Delta G_{exch,gas}^{Lu} = \Delta E_{gas}^{Cr,Lu} - \Delta E_{gas}^{Ru,Lu} \qquad (45)$$

whereby $\Delta E_{gas}^{M,Lu}$ is the electrostatic work required for approaching the spherical Lu^{3+} cation from the charged d-block cation located in the octahedral site of the receptor $[M(\mathbf{L9})_3]^{z+}$ ($M = Cr^{3+}$, Ru^{2+}).[42] A rough point charge model neglecting polarization effects leads to the simple application of the Coulomb law (eqn (46)) for estimating this electrostatic work $\Delta E_{calcd}^{M,Lu}$, whereby N_{Av} is Avogadro's number = 6.023×10^{23} mol^{-1}, z_M and z_{Lu} are the charge of the interacting particles in electrostatic units, e is the elementary charge = 1.602×10^{-19} C, ε_0 is the vacuum permittivity constant = 8.859×10^{-12} C N^{-1} m^{-2}, ε_r is the relative

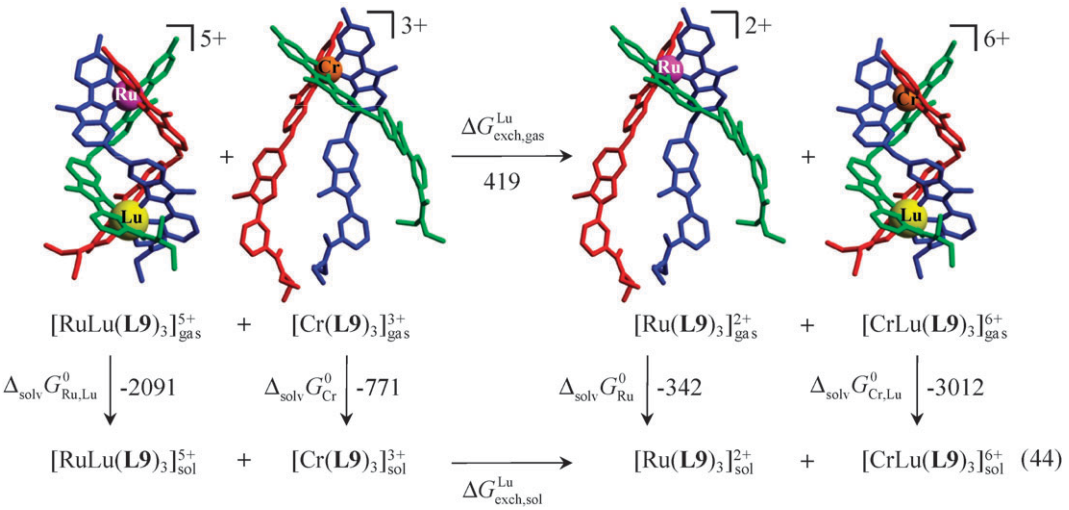

Fig. 15 Thermodynamic Born–Haber cycle for the exchange of Lu^{3+} between the trigonal receptors $[Ru(\mathbf{L9})_3]^{2+}$ and $[Cr(\mathbf{L9})_3]^{3+}$ (Ru^{2+} = purple, Cr^{3+} = orange, Lu^{3+} = yellow; the numerical values are given in kJ mol^{-1}).

dielectric permittivity of the medium and $d_{M,Lu}$ is the intermetallic distance in the binuclear helicate $[MLu(\mathbf{L9})_3]^{(3+z)+}$ (M = Cr, Ru).

$$\Delta E^{M,Lu}_{calcd} = -\frac{N_{Av} z_M z_{Lu} e^2}{4\pi\varepsilon_0} \int_{\infty}^{d_{M,Lu}} \frac{dr}{\varepsilon_r r^2} \qquad (46)$$

Taking $\varepsilon_r \approx 1.0$ within atoms and molecules[43] provides the straightforward integration of eqn (46) to give eqn (47), from which we compute $\Delta E^{Ru,Lu}_{gas} = 918$ kJ mol^{-1} and $\Delta E^{Cr,Lu}_{gas} = 1337$ kJ mol^{-1} by using $z_{Ru} = 2$, $z_{Cr} = z_{Lu} = 3$, $d_{RuLu} = 9.08 \times 10^{-10}$ m,[44] and $d_{CrLu} = 9.35 \times 10^{-10}$ m.[45]

$$\Delta E^{M,Lu}_{gas} = \frac{N_{Av} z_M z_{Lu} e^2}{4\pi\varepsilon_0 d_{M,Lu}} \qquad (47)$$

Introducing these values into eqn (45) gives $\Delta G^{Lu}_{exch,gas} = 419$ kJ mol^{-1} (Fig. 15 top). Interestingly, the various solvation energies $\Delta_{solv}G^0_M$ (for the trigonal receptors $[M(\mathbf{L9})_3]^{z+}$) and $\Delta_{solv}G^0_{M,Lu}$ (for the binuclear helicates $[MLu(\mathbf{L9})_3]^{(3+z)+}$) can be also roughly estimated by using an analytical formulation proposed by Born in eqn (48), whereby Z is the total charge of the complex considered as a uniformally charged sphere of radius R transferred from the vacuum into a dielectric continuum of relative permittivity ε_r.[46]

$$\Delta_{solv}G^0 = -\frac{N_{Av} Z^2 e^2}{8\pi\varepsilon_0 R}\left(1 - \frac{1}{\varepsilon_r}\right) \qquad (48)$$

(i) Introducing $\varepsilon_r = 36.1$ for acetonitrile into eqn (48), (ii) taking R as the pseudo-spherical hydrodynamic radii determined by diffusional NMR for $[M(\mathbf{L9})_3]^{z+}$, $[MLu(\mathbf{L9})_3]^{(3+z)+}$,[42,46] and (iii) neglecting the possible formation of ion pairs, eventually give the solvation energies collected in Fig. 15,[42] from which $\Delta G^{Lu}_{exch,sol}$ can be easily obtained with the help of the Born–Haber cycle.

$$\begin{aligned}\Delta G^{Lu}_{exch,sol} &= \Delta G^{Lu}_{exch,gas} \\ &\quad + (\Delta_{solv}G^0_{Ru} + \Delta_{solv}G^0_{Cr,Lu} - \Delta_{solv}G^0_{Cr} - \Delta_{solv}G^0_{Ru,Lu}) \\ &= 419 - 492 = -73 \text{ kJ mol}^{-1} \end{aligned} \qquad (49)$$

One immediately notices that $\Delta G^{Lu}_{exch,sol}$ corresponds to a balance between two huge, but opposite contributions. The first one is repulsive and results from the standard coulombic interactions between pairs of metallic cations, which globally disfavors the formation of $[CrLu(\mathbf{L9})_3]^{6+}$ over $[RuLu(\mathbf{L9})_3]^{5+}$. This trend is essentially annihilated by the difference in solvation energies, which favors the formation of the products $[Ru(\mathbf{L9})_3]^{2+}$ and $[CrLu(\mathbf{L9})_3]^{6+}$ over the reactants $[Cr(\mathbf{L9})_3]^{3+}$ and $[RuLu(\mathbf{L9})_3]^{5+}$ (eqn (49), Fig. 15). This prediction is confirmed by the experimental thermodynamic stability constants obtained for the formation of $[RuLu(\mathbf{L9})_3]^{5+}$ (equilibrium (50)) and $[CrLu(\mathbf{L9})_3]^{6+}$ (equilibrium (51)) in acetonitrile.[42]

$$[Ru(\mathbf{L9})_3]^{2+} + [Lu(CH_3CN)_9]^{3+} \rightleftharpoons [RuLu(\mathbf{L9})_3]^{5+} + 9\ CH_3CN:\ \log(\beta^{Ru\mathbf{L9},Lu}_{1,1}) = 5.2(2) \qquad (50)$$

$$[Cr(\mathbf{L9})_3]^{3+} + [Lu(CH_3CN)_9]^{3+} \rightleftharpoons [CrLu(\mathbf{L9})_3]^{6+} + 9\ CH_3CN:\ \log(\beta^{Cr\mathbf{L9},Lu}_{1,1}) = 5.3(3) \qquad (51)$$

We deduce $\Delta G^{Lu}_{exch,sol} = -2.30RT[\log(\beta^{Cr\mathbf{L9},Lu}_{1,1}) - \log(\beta^{Ru\mathbf{L9},Lu}_{1,1})] = \Delta E^{Cr,Lu}_{sol} - \Delta E^{Ru,Lu}_{sol} = -0.6(9)$ kJ mol^{-1}, a value close to zero in agreement with the predicted compensation between intermetallic repulsions and solvation effects.[42] This energetic balance operating in solution is a general trend for the homo-component interactions $\Delta E^{\mathbf{L},\mathbf{L}}$ and $\Delta E^{M,M}$, which strongly limits their magnitude and hence their contribution to the stability of the final polynuclear metallo-supramolecular complexes.[16–19,38,47] However, the homo-component interactions may have decisive influence on stability constants, especially when the number of primary hetero-component interactions are equal in the reactants and in the products. In this context, our recurrent dimerization process shown in equilibrium (16) is a striking example because we count twelve hetero-component Ga–**L4**(binding site) connections in the reactants and in the products (see Fig. 12).

$$2\ [Ga_2(\mathbf{L4})_3]^{6-} \rightleftharpoons [Ga_4(\mathbf{L4})_6]^{12-}:\ \beta^{Ga,\mathbf{L4}}_{dim} \qquad (16)$$

The explicit consideration of the homo-component interactions $u^{\mathbf{L4},\mathbf{L4}} = e^{-(\Delta E^{\mathbf{L4},\mathbf{L4}}/RT)}$, $u^{Ga,Ga}_{2,3} = e^{-(\Delta E^{Ga,Ga}_{2,3}/RT)}$, and $u^{Ga,Ga}_{4,6} = e^{-(\Delta E^{Ga,Ga}_{4,6}/RT)}$ transforms eqn (25) and (26) into eqn (52) and (53), from which eqn (54) can be easily deduced by using Kuhn's theory with the same hypotheses and approximations which lead to eqn (28) (see section 4).

$$\beta^{Ga,\mathbf{L4}}_{2,3} = 1536(f^{Ga,\mathbf{L4}}_{inter})^6 (EM^{Ga,\mathbf{L4}}_{2,3})^2 (u^{\mathbf{L4},\mathbf{L4}})^6 (u^{Ga,Ga}_{2,3}) \qquad (52)$$

$$\beta^{Ga,\mathbf{L4}}_{4,6} = 3528944(f^{Ga,\mathbf{L4}}_{inter})^{12} (EM^{Ga,\mathbf{L4}}_{4,6})^3 (u^{\mathbf{L4},\mathbf{L4}})^{12} (u^{Ga,Ga}_{4,6})^6 \qquad (53)$$

$$\begin{aligned}\beta^{Ga,\mathbf{L4}}_{dim} &= \frac{\beta^{Ga,\mathbf{L4}}_{4,6}}{(\beta^{Ga,\mathbf{L4}}_{2,3})^2} = \frac{0.58}{EM^{Ga,\mathbf{L4}}_{2,3}} \frac{(u^{Ga,Ga}_{4,6})^6}{(u^{Ga,Ga}_{2.3})^2} \\ &= \frac{0.58}{EM^{Ga,\mathbf{L4}}_{2,3}} e^{-\left(\frac{6\Delta E^{Ga,Ga}_{4,6} - 2\Delta E^{Ga,Ga}_{2,3}}{RT}\right)} \end{aligned} \qquad (54)$$

From eqn (54), coordination chemists would intuitively set $\Delta E^{Ga,Ga}_{2,3} \approx \Delta E^{Ga,Ga}_{4,6} = \Delta E^{Ga,Ga}$ because the intermetallic separation is almost identical in the triple-stranded helicate $[Ga_2(\mathbf{L4})_3]^{6-}$ and in the tetranuclear cage $[Ga_4(\mathbf{L4})_6]^{12-}$ ($d_{2,3} \approx d_{4,6}$, Fig. 12).[23] This would result in homo-component interactions systematically favoring the formation of the triple-stranded helicates possessing a smaller number of intermetallic interactions. However, this approach has no theoretical support since it relies on the sole consideration of the coulombic repulsion in $\Delta E^{Ga,Ga}_{2,3}$ and $\Delta E^{Ga,Ga}_{4,6}$. The contribution of the solvation energies $\Delta_{solv}G^0_{4,6} - 2\Delta_{solv}G^0_{2,3}$ has to be taken into account, and it requires the determination of the pseudo-spherical radii $R_{2,3}$ and $R_{4.6}$ for the two complexes (Fig. 16).

The consideration of the rough Coulomb approach (eqn (47)) for modeling intermetallic repulsions and of Born eqn (48) for estimating the solvation energies leads to the Born–Haber cycle shown in Fig. 16. Assuming that the effective molarity is identical for the complexation processes operating in the gas-phase and in solution leads to eqn (55), in

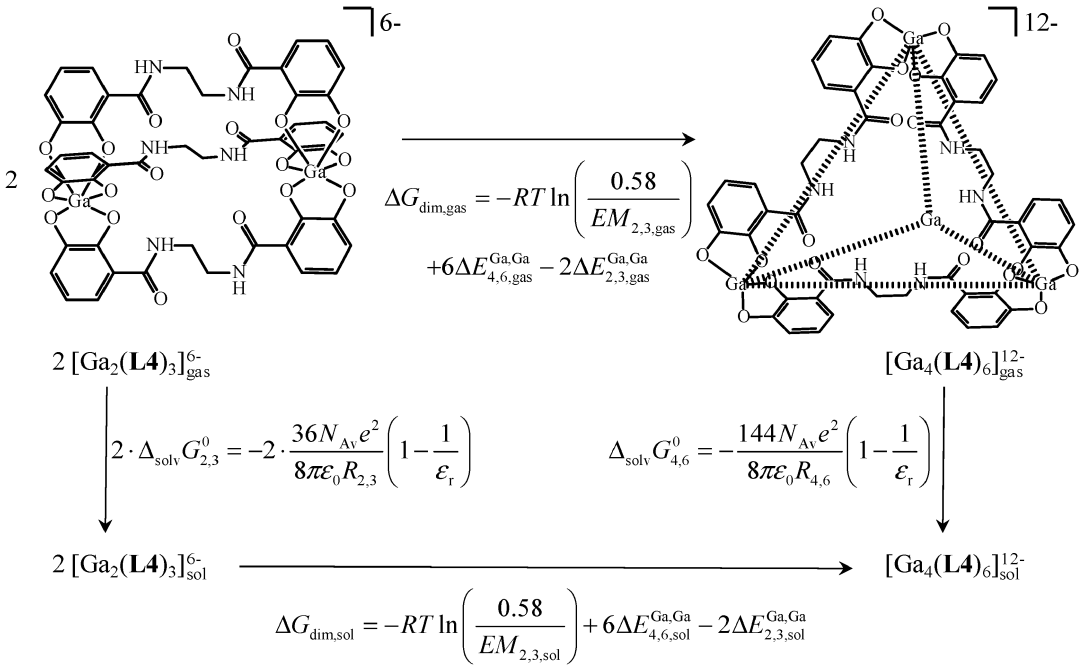

Fig. 16 Putative thermodynamic Born–Haber cycle for the dimerization of $[Ga_2(\mathbf{L4})_3]^{6-}$ to give $[Ga_4(\mathbf{L4})_6]^{12-}$.

which the crucial term $6\Delta E^{\mathrm{Ga,Ga}}_{4,6} - 2\Delta E^{\mathrm{Ga,Ga}}_{2,3\mathrm{sol}}$ can be estimated from four accessible geometric parameters: $d_{2,3}$, $d_{4,6}$, $R_{2,3}$ and $R_{4,6}$.

$$6\Delta E^{\mathrm{Ga,Ga}}_{4,6,\mathrm{sol}} - 2\Delta E^{\mathrm{Ga,Ga}}_{2,3,\mathrm{sol}} = \frac{18N_{\mathrm{Av}}e^2}{4\pi\varepsilon_0}\left(\frac{3}{d_{4,6}} - \frac{1}{d_{2,3}}\right) + \frac{72N_{\mathrm{Av}}e^2}{8\pi\varepsilon_0}\left(1-\frac{1}{\varepsilon_r}\right)\left(\frac{1}{R_{2,3}} - \frac{2}{R_{4,6}}\right) \quad (55)$$

Since it is well-established that the triple-stranded helicates $[Ga_2(\mathbf{L4})_3]^{6-}$ [14*l*,48] and the tetrahedral cages $[Ga_4(\mathbf{L4})_6]^{12-}$ [49] incorporate counter-cations within their endocyclic cavities, the simple use of Born equation for the 'empty' anionic complex is debatable, and no attempt has been made for computing numerical values with eqn (55). Nevertheless, the emerging concept of two gladiators (electrostatic repulsion and solvation energies) fighting with specific weapons (*i.e.* the charge distribution within the metallo-supramolecular complex, the molecular shape and the organization in solution) is crucial for (i) the rationalization of the limited magnitude of the homo-component interactions and (ii) the deliberate manipulation of these contributions for stabilizing (or destabilizing) one specific complex in a thermodynamic self-assembly (see next section). It is worth stressing here that there is no fundamental principle of homo-component interactions that dictate their favorable ($\Delta E^{\mathrm{L,L}} < 0$ or $\Delta E^{\mathrm{M,M}} < 0$, *i.e.* positive cooperativity) or unfavorable ($\Delta E^{\mathrm{L,L}} > 0$ or $\Delta E^{\mathrm{M,M}} > 0$, *i.e.* negative cooperativity) contributions to the global free energy change accompanying the assembly process. The first numerical application in the following section illustrates both cases of positive and negative deviations brought by intramolecular intermetallic interactions.

6. Some attempts for a rational and quantitative use of the five microscopic thermodynamic describers

Since the original efforts focused on the understanding and on the thermodynamic modeling of the formation of the double-stranded helicate $[Cu_3(\mathbf{L1})_2]^{3+}$ (Fig. 1d),[12*b*,15*b*,16*a*,18*b*] we would like to first illustrate the rational use of the five microscopic thermodynamic describers for the unravelling of the closely related diastereoselective self-assembly of the binuclear double-stranded $[M_2(\mathbf{L}k)_2]^{2+}$ helicates (M = Cu^I, Ag^I; $\mathbf{L}k$ = **L10**–**L12**, Fig. 17).[50] Reaction of the most extended bis-bidentate ligand **L12** with increasing amounts of $M(ClO_4)$ in dichloromethane/acetonitrile provides the C_2-symmetrical precursor $[M(\mathbf{L12})_2]^+$ (equilibrium (56) modeled with eqn (57)), followed by the fixation of a second metal to yield the target double stranded-helicate $[M_2(\mathbf{L12})_2]^{2+}$ (equilibrium (58) modeled with eqn (59)).[50*b*]

$$[M(CH_3CN)_4]^+ + 2\ \mathbf{L}k \rightleftharpoons [M(\mathbf{L}k)_2]^+ + 4\ CH_3CN\ \beta^{\mathrm{M,L}k}_{1,2} \quad (56)$$

$$\beta^{\mathrm{M,L}k}_{1,2} = 12(f^{\mathrm{M}}_{\mathrm{N2}})^2 u^{\mathrm{L}k,\mathrm{L}k} \quad (57)$$

$$2\,[M(CH_3CN)_4]^+ + 2\ \mathbf{L}k \rightleftharpoons [M_2(\mathbf{L}k)_2]^{2+} + 8\ CH_3CN:\ \beta^{\mathrm{M,L}k}_{2,2} \quad (58)$$

$$\beta^{\mathrm{M,L}k}_{2,2} = 72(f^{\mathrm{M}}_{\mathrm{N2}})^4 (EM^{\mathrm{M,L}k})(u^{\mathrm{L}k,\mathrm{L}k})^2 (u^{\mathrm{M,M}}_{\mathrm{L}k}) \quad (59)$$

For the less extended ligands **L10** and **L11**, the associated double-stranded helicates $[M_2(\mathbf{L}k)_2]^{2+}$ (equilibrium (58)) are the only species detected by spectrophotometry for Ln : $\mathbf{L}k \leq 2.0$, while $[M_2(\mathbf{L}k)]^{2+}$ are formed in excess of metal (equilibrium (60) modeled with eqn (61)).[50*b*]

$$2\,[M(CH_3CN)_4]^+ + \mathbf{L}k \rightleftharpoons [M_2(\mathbf{L}k)]^{4+} + 8\ CH_3CN:\ \beta^{\mathrm{M,L}k}_{2,1} \quad (60)$$

$$\beta^{\mathrm{M,L}k}_{2,1} = 144(f^{\mathrm{M}}_{\mathrm{N2}})^2 (u^{\mathrm{M,M}}_{\mathrm{L}k}) \quad (61)$$

In summary, six experimental stability constants can be collected for the complexation of each metal (M = Cu^{I} or Ag^{I}) with the three ligands ($\beta_{2,2}^{M,L10}$, $\beta_{2,1}^{M,L10}$, $\beta_{2,2}^{M,L11}$, $\beta_{2,1}^{M,L11}$, $\beta_{1,2}^{M,L12}$, $\beta_{2,2}^{M,L12}$, equilibria (56), (58) and (60)), while ten microscopic parameters are required for their thermodynamic modeling (f_{N2}^{M}, $EM^{M,L10}$, $EM^{M,L11}$, $EM^{M,L12}$, $u^{L10,L10}$, $u^{L11,L11}$, $u^{L12,L12}$, $u_{L10}^{M,M}$, $u_{L11}^{M,M}$, $u_{L12}^{M,M}$, eqn (57), (59) and (61)). For reducing the number of fitted parameters to a maximum of six, the following reasonable hypotheses were applied: (i) the interligand interaction is identical for any [M(bipyridine)$_2$] units ($u^{L,L} = u^{L10,L10} = u^{L11,L11} = u^{L12,L12}$) and (ii) the second ligand strand, responsible for the intramolecular connection in $[M_2(\mathbf{Lk})_2]^{2+}$, is considered as a flexible optimized jointed chain for which eqn (24) holds ($EM^{M,Lk} = EM^{M,L10}\,(a^{Lk}/a^{L10})^{-3}$). Multi-linear least-squares fits of the 6 experimental stability constants with eqn (57), (59) and (61), eventually allow the estimation of the six microscopic parameters collected in Table 3.[50b]

As expected, $\Delta G_{N2}^{Cu} < \Delta G_{N2}^{Ag}$ confirms the well-established preference of the bidentate bipyridine binding unit for Cu^{I} with respect to Ag^{I}.[51] Interestingly, the interligand interactions accompanying the successive fixation of two bipyridine units to the same metal are significantly repulsive ($9 \leq \Delta E^{L,L} \leq 20$ kJ mol^{-1}, Table 3), which strongly contributes to the global anti-cooperative assembly of the double-stranded helicates $[M_2(\mathbf{Lk})_2]^{2+}$. The experimental effective molarities ($1.5 \leq EM_{a=13.9Å}^{M,L10} \leq 5.0$ M; $0.7 \leq EM_{a=18.2Å}^{M,L11} \leq 2.2$ M; and $0.4 \leq EM_{a=22.3Å}^{M,L12} \leq 1.2$ M, Table 3) are large, which implies a remarkable preorganization of the ligand strand for the intramolecular connection leading to the macrocyclic double-stranded helicates. However, the most striking point concerns

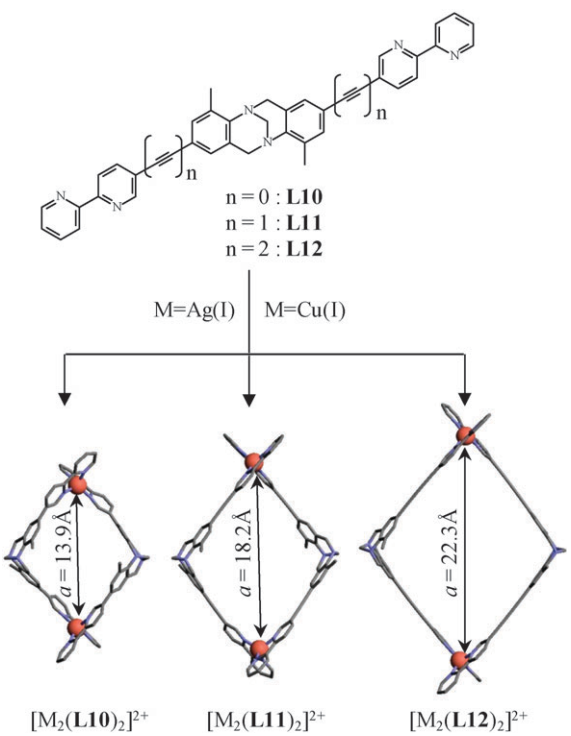

Fig. 17 Diastereoselective formation of the double-stranded helicates $[M_2(\mathbf{Lk})_2]^{2+}$ (M = Cu^{I}, Ag^{I}; **Lk** = **L10**–**L12**; adapted from ref. 50*b*).

Table 3 Fitted microscopic thermodynamic parameters for the self-assembly of $[M_m(\mathbf{Lk})_n]^{m+}$ (M = Cu^{I}, Ag^{I}; k = 10–12) in dichloromethane–acetonitrile (5 : 1) at 293 K[50]

Microscopic parameters	M = Cu(I)	M = Ag(I)
$\log(f_{N2}^{M})/\Delta G_{N2}^{M}$ [a]	6.6/−38	4.3/−25
$\log(EM^{M,L10})/\Delta G_{corr}^{M,L10}$ [b]	0.18/−1	0.7/−4
$\log(u^{L,L})/\Delta E^{L,L}$ [c]	−3.5/20	−1.6/9.4
$\log(u_{L10}^{M,M})/\Delta E_{L10}^{M,M}$ [d]	−2/11	2.5/−14
$\log(u_{L11}^{M,M})/\Delta E_{L11}^{M,M}$ [d]	−3.5/20	−0.4/2.4
$\log(u_{L12}^{M,M})/\Delta E_{L12}^{M,M}$ [d]	−5.7/33	−3.9/22

[a] $\Delta G_{N2}^{M} = -2.303RT\log(f_{N2}^{M})$ kJ mol^{-1}. [b] $\Delta G_{corr}^{M,L10} = -2.303RT\log(EM^{M,L10})$ kJ mol^{-1}. [c] $\Delta E^{L,L} = -2.303RT\log(u^{L,L})$ kJ mol^{-1}. [d] $\Delta E_{Lk}^{M,M} = -2.303RT\log(u_{Lk}^{M,M})$ kJ mol^{-1}.

the globally repulsive intermetallic interactions, which indeed become larger with increasing intermetallic separations ($\Delta E_{L10,a=13.4Å}^{M,M} < \Delta E_{L11,a=18.2Å}^{M,M}$ () $< \Delta E_{L12,a=22.3Å}^{M,M}$, Table 3), an observation in strong contrast with common chemical intuitions solely based on electrostatic Coulomb interactions. Quantitatively speaking, the latter effect is responsible for 90% of the decrease in stability on going from $[M_2(\mathbf{L10})_2]^{2+}$ to $[M_2(\mathbf{L11})_2]^{2+}$ and finally to $[M_2(\mathbf{L12})_2]^{2+}$, the remaining 10% contribution being assigned to the decrease of EM with increasing intermetallic separation. This counter-intuitive observation can be justified by the consideration of the balance between the opposite effects of (i) the repulsive intermetallic coulombic repulsion resulting from the fixation of the second cation at a distance a and (ii) the favorable solvation of the double-stranded helicate $[M_2(\mathbf{Lk})_2]^{2+}$, which is reduced when a increases (Fig. 18).[50b] Altogether, the second effect dominates in this series of helicates, thus producing apparent anti-coulombic behaviour for the intermetallic interactions measured in solution. The rough structural model shown in Fig. 18 treated with simple Coulomb (eqn (47)) and Born (eqn (48)) equations indeed predicts that $\Delta E_{L11,sol}^{Ag,Ag} > \Delta E_{L10,sol}^{Ag,Ag}$ if one assumes similar solvation energies for ligands **L10** and **L11**, in agreement with experimental data ($\Delta E_{L11,sol}^{Ag,Ag} - \Delta E_{L10,sol}^{Ag,Ag} = 16$ kJ mol^{-1}, Table 3).[50b]

The versatility of $\Delta E_{sol}^{M,M}$, combined with its counter-intuitive contribution to the global stability of self-assembled complexes, stimulated the Geneva's group to patiently collect twenty-nine different thermodynamic stability constants characterizing the formation of single-, double- and triple-stranded helicates obtained for the reaction of Lu^{3+} or Zn^{2+} with a family of segmental ligands possessing only three different types of chelating units: one bidentate (N_2) and two tridentate (N_3 and N_2O) binding sites (Fig. 19, ligands **L7**, **L13**–**L22**).[38,47,52] Because of (i) the very limited number of different binding sites and (ii) the systematic 9 Å intermetallic separation found in the polynuclear $[Lu_{m_1}Zn_{m_2}(\mathbf{Lk})_n]^{(3m_1+2m_2)+}$ helicates, a restricted set of ten microscopic thermodynamic describers is sufficient for modeling the 29 stability constants with eqn (11).[47] A global non-linear least-squares fit allows the satisfying re-calculation of all experimental stability constants by using the ten microscopic parameters collected in Table 4.

First, we notice $EM \approx 10^{-4}$ M for the average effective molarity characterizing the intramolecular macrocyclization process operating between two metals separated by 9 Å in

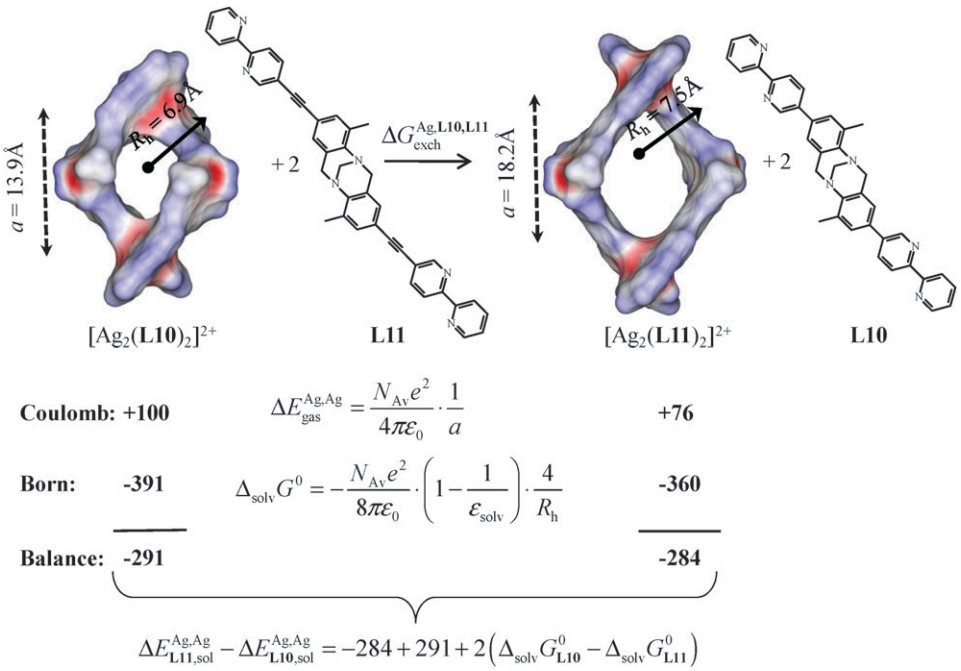

Fig. 18 A rough quantitative analysis of the Coulomb and Born contributions to the apparent homo-component intermetallic interactions operating in solution for the double-stranded helicates $[Ag_2(\mathbf{L10})_2]^{2+}$ and $[Ag_2(\mathbf{L11})_2]^{2+}$ (a is the intermetallic separations, R_h is the pseudo-spherical hydrodynamic radius. Numerical values for the free energies are given in kJ mol^{-1}).[50b]

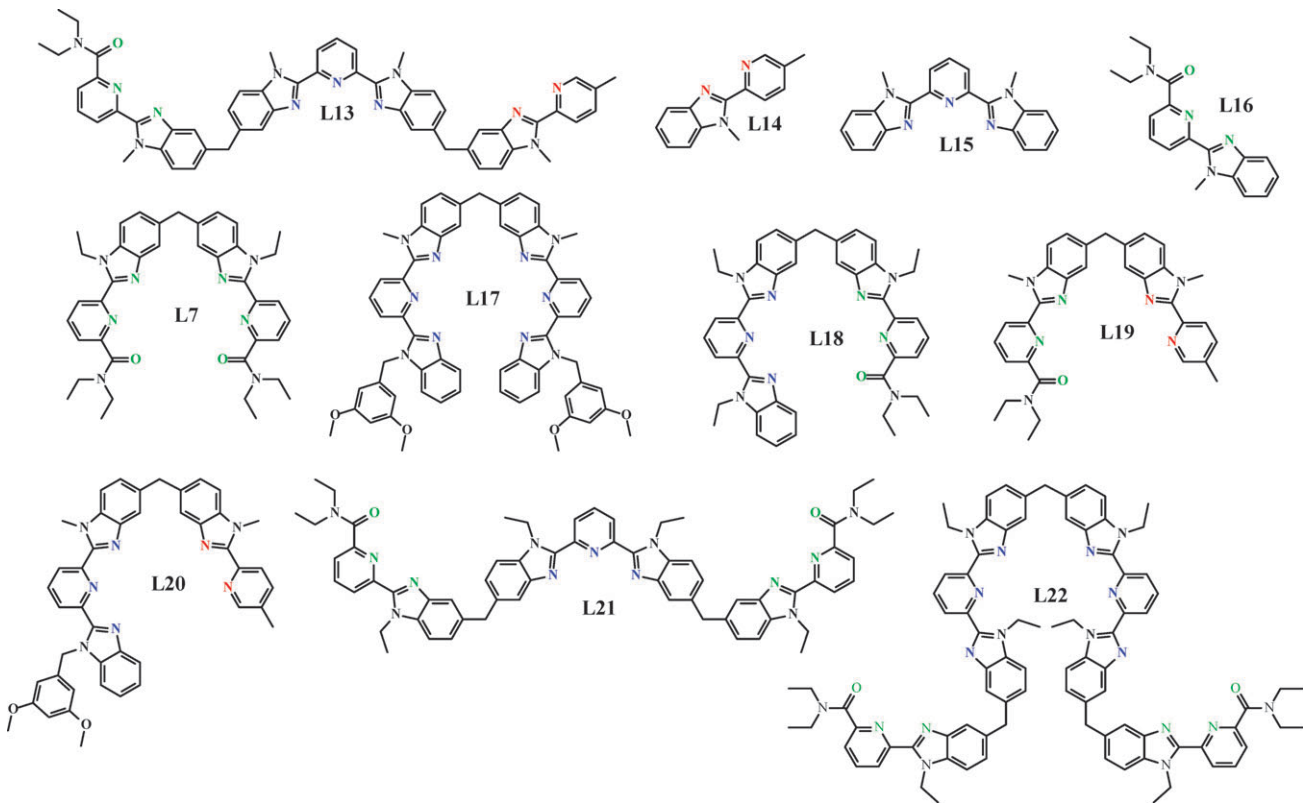

Fig. 19 Structures of the ligands **L7**, **L13**–**L22** highlighting the tridentate N_3 (blue), N_2O (green) and the bidentate N_2 (red) binding sites.

these helicates. This is the signature for a limited preorganization of the segmental ligand for the formation of macro(poly)cyclic helicates. However, *EM* remains large enough for avoiding dimerization (eqn (28)) and/or some conversions into larger oligomers which minimize the total number of intramolecular connections. Consequently, only linear helicates could be detected in solution for reactions of ligands **L7**, **L13**–**L22** with Lu^{3+} and Zn^{2+}.[38,47] Again, the most striking result concerns

Table 4 Fitted microscopic thermodynamic describers for $[Lu_{m_1}Zn_{m_2}(\mathbf{L}k)_n]^{(3m_1+2m_2)+}$ (m_1 = 0–3; m_2 = 0, 1; n = 1–3; **L***k* = **L7**, **L13**–**L22**; acetonitrile, 298 K; Δg and ΔE are in kJ mol^{-1}).[47]

Microscopic parameters	
$\log(f_{N_2O}^{Lu,\mathbf{L}k})/\Delta g_{N_2O}^{Lu,\mathbf{L}k}$	5.5(2)/−31(1)
$\log(f_{N_3}^{Lu,\mathbf{L}k})/\Delta g_{N_3}^{Lu,\mathbf{L}k}$	5.3(2)/−30(1)
$\log(f_{N_2}^{Zn,\mathbf{L}k})/\Delta g_{N_2}^{Zn,\mathbf{L}k}$	7.0(3)/−40(1)
$\log(EM)/\Delta g_{corr}^{M,\mathbf{L}k}$	−3.9(4)/23(2)
$\log(u^{\mathbf{L},\mathbf{L}})/\Delta E^{\mathbf{L},\mathbf{L}}$	−0.1(3)/1(2)
$\log(u_{1-2}^{Lu,Lu})/\Delta E_{1-2}^{Lu,Lu}$[a]	−0.6(3)/4(1)
$\log(u_{1-2}^{Zn,Lu})/\Delta E_{1-2}^{Zn,Lu}$[a]	−3.1(3)/18(2)
$\log(u_{1-3}^{Lu,Lu})/\Delta E_{1-3}^{Lu,Lu}$[a]	1.4(7)/−8(3)
$\log(u_{1-3}^{Zn,Lu})/\Delta E_{1-3}^{Zn,Lu}$[a]	0.8(6)/−4(2)
$\log(u_{1-4}^{Lu,Lu})/\Delta E_{1-4}^{Lu,Lu}$[a]	−3.2(8)/18(4)

[a] The subscript indexes indicate geminal (1–2, d = 9 Å), vicinal (1–3, d = 18 Å) and long-range (1–4, d = 27 Å) intermetallic interactions along the helical axis (see Fig. 20).

the counter-intuitive evolution of the apparent intermetallic interactions operating in solution ($\Delta E_{d=27Å}^{Lu,Lu} > \Delta E_{d=9Å}^{Lu,Lu} > \Delta E_{d=18Å}^{Lu,Lu}$ and $\Delta E_{d=9Å}^{Zn,Lu} > \Delta E_{d=9Å}^{Lu,Lu}$, Table 4 and Fig. 20), which can be rationalized by taking into account the opposite contributions of coulombic repulsions and solvation energies.[47]

By chance, the geometrical characteristics of the triple-stranded helicates $[Lu_{m_1}Zn_{m_2}(\mathbf{L}k)_n]^{(3m_1+2m_2)+}$ (**L***k* = **L7**, **L13**–**L22**) produce almost complete compensation between coulombic repulsions and solvation energies, which allows the formation of stable highly charged complexes. Moreover, the exclusive resort to analytical formulations for the Coulomb and Born equations allowed the derivation of explicit mathematical expressions for $\Delta E_{1-2}^{Lu,Lu}$, $\Delta E_{1-3}^{Lu,Lu}$, $\Delta E_{1-4}^{Lu,Lu}$, $\Delta E_{1-2}^{Zn,Lu}$ and $\Delta E_{1-3}^{Zn,Lu}$ (eqn (62)–(66), whereby d is the geminal intermetallic distance, αd is the expansion coefficient measuring the increase in pseudo-spherical hydrodynamic radius upon fixation of an additional metal, $R_h^{ML_3}$ is the pseudo-spherical hydrodynamic radius of the precursor complex $[ML_3]^{z+}$, the other terms having their usual meaning).[47]

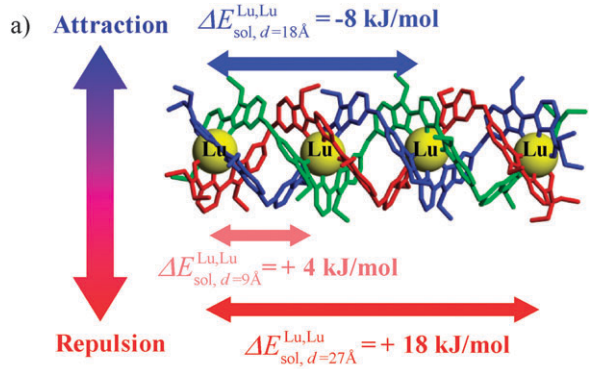

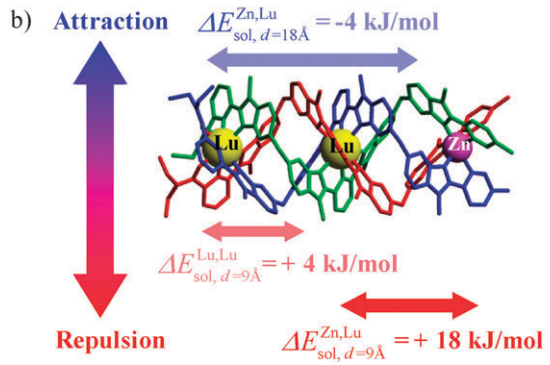

Fig. 20 Experimental intermetallic interactions operating within the triple-stranded helicates in solution: (a) $[Lu_4(\mathbf{L22})_3]^{12+}$ and (b) $[Lu_2Zn(\mathbf{L13})_3]^{8+}$ (CH_3CN, 298 K).[47]

$$\Delta E_{1-2}^{Lu,Lu} = \frac{(z_{Lu})^2 e^2 N_{Av}}{4\pi\varepsilon_0}\left(\frac{1}{d} - \frac{1}{R_0^{Lu(\mathbf{L22})_3}}\left(1-\frac{1}{\varepsilon_r}\right)\left(\frac{(1-\alpha d)}{(1+\alpha d)}\right)\right) + 3\Delta_{solv}G_{\mathbf{L22}}^0 \quad (62)$$

$$\Delta E_{1-3}^{Lu,Lu} = \frac{(z_{Lu})^2 e^2 N_{Av}}{4\pi\varepsilon_0} \times \left(\frac{1}{2d} - \frac{1}{R_0^{Lu(\mathbf{L22})_3}}\left(1-\frac{1}{\varepsilon_r}\right)\left(\frac{(\alpha d-1)^2}{(1+\alpha d)(1+2\alpha d)}\right)\right) \quad (63)$$

$$\Delta E_{1-4}^{Lu,Lu} = \frac{(z_{Lu})^2 e^2 N_{Av}}{4\pi\varepsilon_0}\left(\frac{1}{3d} - \frac{1}{R_0^{Lu(\mathbf{L22})_3}}\left(1-\frac{1}{\varepsilon_r}\right) \cdot \left(\frac{(\alpha d-1)^2}{(1+\alpha d)(1+2\alpha d)(1+3\alpha d)}\right)\right) \quad (64)$$

$$\Delta E_{1-2}^{Zn,Lu} = \frac{e^2 N_{Av}}{4\pi\varepsilon_0}\left(\frac{z_{Zn}z_{Lu}}{d} - \frac{1}{2}\left(1-\frac{1}{\varepsilon_r}\right) \cdot \left(-\frac{2(z_{Zn})^2}{R_0^{Zn(\mathbf{L13})_3}} + \frac{(z_{Zn}+z_{Lu})^2}{R_0^{Zn(\mathbf{L13})_3}(1+\alpha d)} - \frac{(z_{Lu})^2}{R_0^{Lu}} + \frac{(z_{Zn})^2}{R_0^{Zn}}\right)\right) + 3\Delta_{solv}G_{\mathbf{L13}}^0 - RT\ln(4) \quad (65)$$

$$\Delta E_{1-3}^{Zn,Lu} = \Delta E_{1-2}^{Zn,Lu} - \Delta E_{1-2}^{Lu,Lu} + \frac{e^2 N_{Av}}{4\pi\varepsilon_0}\left(\frac{(z_{Lu})^2}{d} - \frac{(z_{Lu}z_{Zn})}{2d} - \frac{1}{2R_0^{Zn(\mathbf{L13})_3}}\left(1-\frac{1}{\varepsilon_r}\right) \times \left(-\frac{2(z_{Lu}+z_{Zn})^2}{(1+\alpha d)} + \frac{(2z_{Lu}+z_{Zn})^2}{(1+2\alpha d)} + (z_{Zn})^2\right)\right) \quad (66)$$

Though the latter equations may frighten synthetic coordination chemists, they indeed depend on a very limited set of addressable geometrical parameters, and can be used for highlighting the trends in stability brought by the contribution of intermetallic interactions upon deliberate structural design. Let's consider three different structural modulations. (1) The triply charged Lu^{3+} cations are replaced with Ca^{2+} to give the hypothetical complex $[Ca_4(\mathbf{L22})_3]^{8+}$, all other parameters

being kept. The intermetallic contributions are obtained by introducing $z_{Lu} = 2$ in eqn (62)–(64), and one predicts that the solvation energies should massively overcome coulombic interactions at short distances (Fig. 21a).[47]

(2) On the contrary, a 22% contraction of the intermetallic separations in the tetranuclear lutetium helicate, modeled with the use of $d = 7$ Å and $R_0^{Lu(\mathbf{L22})_3} = 10$ Å in eqn (62)–(64) (instead of $d = 9$ Å and $R_0^{Lu(\mathbf{L22})_3} = 13$ Å found for $[Lu_4(\mathbf{L22})_3]^{12+}$) favors electrostatic coulombic repulsions to such an extent, that only repulsive intermetallic interactions are expected (Fig. 21b).[47] (3) Finally, a significant increase in rigidity of the triple-helical scaffold modeled by reducing αd from 8.2% (found in $[Lu_4(\mathbf{L22})_3]^{12+}$) to 5% shows a drastic domination of solvation energies, even for long-range intermetallic interactions (Fig. 21c).[47]

The effective molarity, *EM*, is also amenable to deliberate manipulation *via* the introduction of controlled ring constraints operating during the two successive intramolecular macrocyclization processes leading to the binuclear triple-stranded helicates $[Ln_2(\mathbf{L7})_3]^{6+}$ and $[Ln_2(\mathbf{L23})_3]$ (Fig. 22).[52] The cumulative stability constant for the formation of a triple-stranded

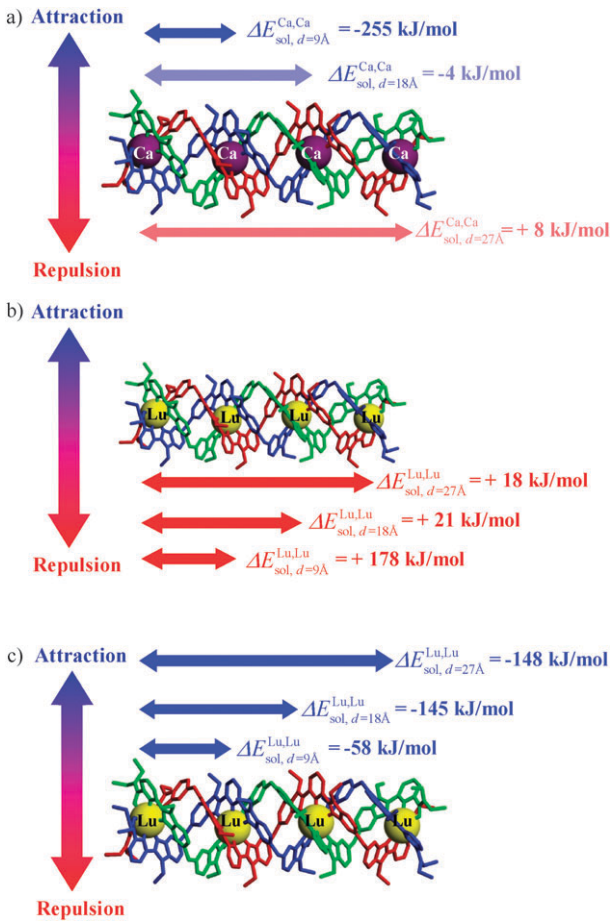

Fig. 21 Intermetallic interactions predicted with eqns (62)–(64) for some putative tetranuclear triple-stranded helicates in acetonitrile: (a) $[Ca_4(\mathbf{L22})_3]^{8+}$ ($z_{Lu} = 2$, $d = 9$ Å, $\alpha d = 8.2\%$, $R_0^{Lu(\mathbf{L22})_3} = 13$ Å, see text), (b) $[Lu_4(\mathbf{L22})_3]^{12+}$ ($z_{Lu} = 3$, $d = 7$ Å, $\alpha d = 8.2\%$, $R_0^{Lu(\mathbf{L22})_3} = 10$ Å, see text) and (c) $[Lu_4(\mathbf{L22})_3]^{12+}$ ($z_{Lu} = 3$, $d = 9$ Å, $\alpha d = 5\%$, $R_0^{Lu(\mathbf{L22})_3} = 13$ Å, see text).[47]

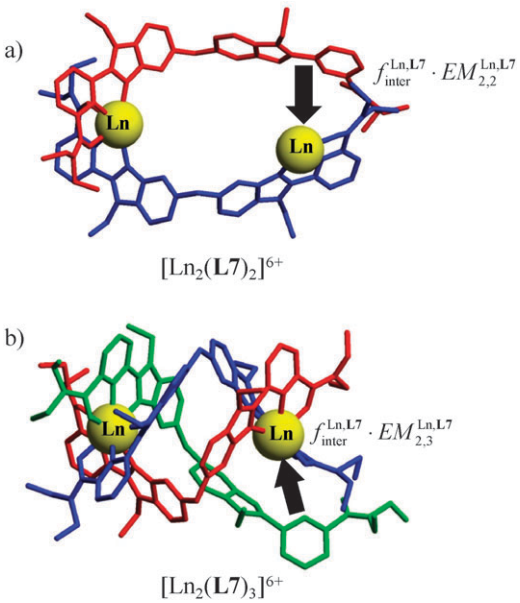

Fig. 22 Schematic illustration of the two successive intramolecular connections leading to (a) $[Ln_2(\mathbf{L7})_2]^{6+}$ and (b) $[Ln_2(\mathbf{L7})_3]^{6+}$.

helicate has been already modeled in eqn (13), a mathematical expression which also holds for $[Ln_2(\mathbf{L7})_3]^{6+}$ and $[Ln_2(\mathbf{L23})_3]$ when the statistical factor is adapted for nine-coordinate lanthanides (eqn (67)).[53]

$$\beta_{2,3}^{Ln,\mathbf{Lk}} = 96(f_{inter}^{Ln,\mathbf{Lk}})^6(EM_{2,2}^{Ln,\mathbf{Lk}})(EM_{2,3}^{Ln,\mathbf{Lk}})(u^{Ln,Ln})(u^{\mathbf{Lk},\mathbf{Lk}})^6 \quad (67)$$

However, the five different microscopic thermodynamic descriptors involved in eqn (67) requires a minimal set of six independent equations associated with six experimental stability constants, while only five are available when one considers the formation of $[Ln_2(\mathbf{L7})_3]^{6+}$ or $[Ln_2(\mathbf{L23})_3]$ (eqn (67)), together with the formation of the double-stranded intermediates $[Ln_2(\mathbf{L7})_2]^{6+}$ or $[Ln_2(\mathbf{L23})_2]^{2+}$ (eqn (68)) and the coordination of the respective precursors with a single metal in $[Ln(\mathbf{L6})_n]^{3+}$ and in $[Ln(\mathbf{L24})_n]^{(3-n)+}$ ($n = 1$–3, eqn (69)–(71) and Fig. 23).[52]

$$\beta_{2,2}^{Ln,\mathbf{Lk}} = 72(f_{inter}^{Ln,\mathbf{Lk}})^4(EM_{2,2}^{Ln,\mathbf{Lk}})(u^{Ln,Ln})(u^{\mathbf{Lk},\mathbf{Lk}})^2 \quad (68)$$

$$\beta_{1,1}^{Ln,\mathbf{Lq}} = 6(f_{inter}^{Ln,\mathbf{Lk}}) \quad (69)$$

$$\beta_{1,2}^{Ln,\mathbf{Lq}} = 12(f_{inter}^{Ln,\mathbf{Lk}})^2(u^{\mathbf{Lk},\mathbf{Lk}}) \quad (70)$$

$$\beta_{1,3}^{Ln,\mathbf{Lq}} = 16(f_{inter}^{Ln,\mathbf{Lk}})^3(u^{\mathbf{Lk},\mathbf{Lk}})^3 \quad (71)$$

Taking an average *EM* values for the two successive intramolecular connections $EM_{2,2}^{Ln,\mathbf{Lk}} \simeq EM_{2,3}^{Ln,\mathbf{Lk}} = EM^{Ln,\mathbf{Lk}}$, allows the least-squares fit of eqn (67)–(71) for each ligand **L7** and $[\mathbf{L23}]^{2-}$.[52] Focussing on the fitted effective molarities collected in Table 5, we notice that $EM^{Ln,\mathbf{L7}}$ is very sensitive to the ionic size of the metal. and it decreases by three orders of magnitudes when the ionic radius increases by 15% on going from $[Lu_2(\mathbf{L7})_3]^{6+}$ to $[La_2(\mathbf{L7})_3]^{6+}$. Surprisingly, the reverse trend is observed with $[\mathbf{L23}]^{2-}$, in which two degrees of rotational freedoms has been removed by the introduction of fused aromatic rings in the quinoline moieties (Fig. 23).[52] Moreover, the gain in rigidity on going from **L7** to $[\mathbf{L23}]^{2-}$

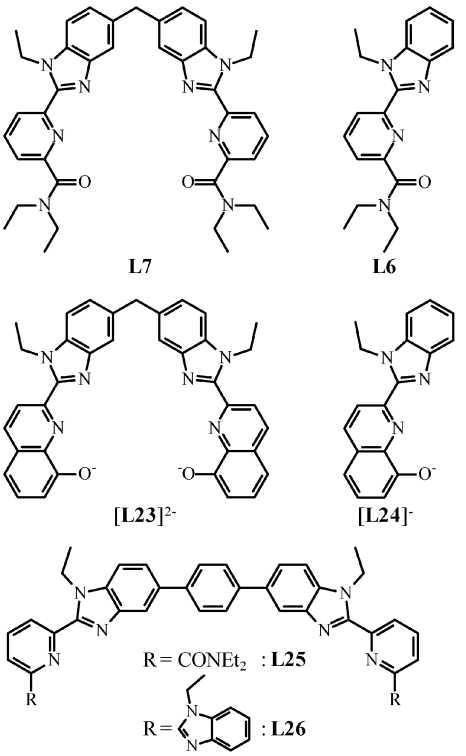

Fig. 23 Chemical structures of the bis-tridentate ligands **L7**, $[\mathbf{L23}]^{2-}$, **L25** and **L26**, and of their tridentate precursors **L6** and $[\mathbf{L24}]^{-}$.

Table 5 Fitted average effective molarities $EM^{\mathrm{Ln},\mathbf{L}k}$ (M) for the formation of the double-stranded $[\mathrm{Ln}_2(\mathbf{L}k)_2]^{6+}$ (k = 25–26), and triple-stranded $[\mathrm{Ln}_2(\mathbf{L7})_3]^{6+}$ and $[\mathrm{Ln}_2(\mathbf{L23})_3]$ helicates (acetonitrile for **L7**, **L25**–**L26** and acetonitrile–methanol 1 : 1 for $[\mathbf{L23}]^{2-}$, 298 K)[52,53]

Ligand	Ln = La	Ln = Eu	Ln = Y	Ln = Lu
L7	$10^{-7.3(1)}$	$10^{-5.5(2)}$	$10^{-6.29(4)}$	$10^{-4.3(1)}$
$[\mathbf{L23}]^{2-}$	$10^{-6.8(1)}$	$10^{-5.83(4)}$	$10^{-9.1(4)}$	$10^{-9.5(5)}$
L25[a]	$10^{-6.3(3)}$	$10^{-5.5(4)}$	$10^{-6.2(1)}$	$10^{-5.5(3)}$
L26[a]	$10^{-8.0(4)}$	$10^{-7.5(4)}$	$10^{-7.4(3)}$	$10^{-6.6(1)}$

[a] The values of EM for ligands **L25** and **L26** correspond to $EM^{\mathrm{Ln},\mathbf{L}k}_{2,2}$ since the triple-stranded helicate cannot be detected in solution.

unambiguously disfavors intramolecular cyclization, thus leading to some extreme values for the effective molarity (*i.e.* $EM^{\mathrm{Lu},\mathbf{L23}} = 10^{-9.5}$ M), which can be attributed to the considerable enthalpic penalty provided by ring strain upon macrocyclization.

In this context, the introduction of a rigid phenyl spacer in ligand **L25** and **L26** produces even larger constraints, which prevent the second macrocyclization and the detection of triple-stranded helicates in solution. In this case, the reported effective molarities strictly correspond to $10^{-8} \leq EM^{\mathrm{Ln},\mathbf{L}k}_{2,2} \leq 10^{-5.5}$ M (k = 25, 26, Table 5), while the upper limit of the effective molarities for the second macrocyclization leading to the triple-helix has been estimated to reach $10^{-14} \leq EM^{\mathrm{Ln},\mathbf{L}k}_{2,3} \leq 10^{-9}$ M (k = 25, 26) along the lanthanide series.[53] In other words, the bis-tridentate ligand **L7**, and its extended versions **L21** (tris-tridentate) and **L22** (tetra-tridentate) are still sufficiently preorganized for the operation of intramolecular bonds leading to macrocyclic linear multi-stranded helicates. The magnitude of the effective molarity is compatible with the quantitative formation of polynuclear triple-stranded helicates at millimolar concentrations under stoichiometric conditions.[38,47] The situation slightly changes for $[\mathbf{L23}]^{-}$, because the smaller effective molarity $EM^{\mathrm{Lu},\mathbf{L23}}$ now prevents the quantitative transformation of the double-stranded $[\mathrm{Ln}_2(\mathbf{L23})_2]^{2+}$ into the triple-stranded helicates $[\mathrm{Ln}_2(\mathbf{L23})_3]$ at millimolar concentration and for $\mathrm{Ln} : [\mathbf{L23}]^{-} = 2 : 3$.[52] The introduction of a rigid aromatic phenyl spacer between the two tridentate binding units in **L25** and **L26** produces even more drastic effects, and the measured effective molarities eventually preclude the formation of the triple-stranded helicates under experimentally accessible conditions.[53] This approach mirrors the ligand design elected by Ward and co-workers[14q,14t] for the preparation of structural alternatives to standard double- and triple-stranded helicates (Fig. 3). Based on the effect of EM on the archetypal dimerization process illustrated in section 4 (eqn (28)), we can conclude that some systematic 'magical' preferences for the formation of complicated d-block or f-block polynuclear clusters, instead of the planned binuclear multiple-stranded helicates, probably originate from the very small magnitudes of the effective molarities produced by the introduction of rigid aromatic spacers between the complexing units. This assumption is supported by the experimental determination of $EM^{\mathrm{Ln},\mathbf{L}k}_{2,2}$ and by the estimation of $EM^{\mathrm{Ln},\mathbf{L}k}_{2,3}$ for the reaction of ligands **L25** and **L26** with trivalent lanthanides.[53]

7. Conclusion and outlook

Among the contributions to the free energy change accompanying the formation of $[\mathrm{M}_{pm}\mathbf{L}_{pn}]$ complexes from their pm M and pn **L** components in solution, those arising from the rotational statistical factor $\Delta g^{\mathrm{stat}}_{pm,pn} = -RT\ln(\omega^{\mathrm{M,L}}_{pm,pn})$ and from the intermolecular metal–ligand affinity $\Delta g^{\mathrm{M,L}}_{pm,pn} = -RT\ln(f^{\mathbf{M,L}}_{\mathrm{inter}})$ are the most familiar to coordination chemists. The first one refers to the unavoidable change in intrinsic rotational entropy produced by the transformation of the reactants into products. It can be easily estimated by using the method of the symmetry numbers once (i) the symmetry point group of each partner contributing to the self-assembly is at hand, and (ii) the internal free rotations operating at room temperature are specified. Chemically speaking, the contribution of this statistical factor to the stability of the final metallo-supramolecular complex is usually small compared to the metal–ligand interactions, but it can be compared with some homo-component perturbations. The free energy of intermolecular connection $\Delta g^{\mathbf{M,L}}_{\mathrm{inter}}$ corresponds to the free energy balance between the breaking of some metal–solvent bonds, which are replaced by the formation of novel metal–ligand bonds connecting two previously independent partners. For each intermolecular bond breaking or bond making process, we expect classical enthalpy/entropy compensation effects,[54] in which the change in bonding order is balanced by some gain (bond breaking) or loss (bond making) of translational entropy.[55] Nevertheless, the contribution of the intermolecular M–**L** connections represents the main force, which drives the self-assembly to

completion. This globally justifies the common use in metallo-supramolecular chemistry of the two well-accepted principles of (i) *maximum site occupancy* (*i.e.* which maximizes the number of favorable intermolecular M–**L** connections) and (ii) *stereochemical matching* (*i.e.* which enthalpically optimizes each specific M–**L** interaction). The chemical interpretation and manipulation of the effective molarity, *EM*, and its consequence on the intramolecular connection is less obvious. Based on a reference state of 1 M, $EM > 1$ M indicates that the intramolecular process becomes more favorable than its intermolecular counterpart. This situation is observed for the formation of complexes with very rigid ligands, which are highly preorganized for a 'strain-free' intramolecular connection leading to the final macrocyclic complex, as found for the toroidal double-stranded helicates $[M_2(\mathbf{L}\boldsymbol{k})_2]^{2+}$ (M = Cu^I, Ag^I; **L*k*** = **L10**–**L12**, Fig. 17).[50] However, the formation of all other studied double-stranded and triple-stranded helicates is characterized by $EM \ll 1$ M, which tends to favor the formation of larger assemblies including more components, but a reduced number of intramolecular connections. Fig. 24 illustrates some selected competitive reactions affecting the assembly of double-stranded helicates, while Fig. 25 holds for triple-stranded helicates. Beyond the minor primary statistical factors (8/9, 1, 3/2 and 27/4) calculated for the selected *n*-merization processes, the contribution of the effective molarities to these equilibria is systematically controlled by the denominator (Fig. 24 and 25). If we assume a single value for *EM* within the two types of complexes related by the *n*-merization equilibrium, we deduce $\beta_{n-\mathrm{mer}} \propto EM^{-\alpha}$ ($\alpha \geq 1$), in agreement with the preferred formation of high-nuclearity complexes with ligand possessing rigid spacers maladjusted for intramolecular macrocyclization, a phenomenon sometimes referred to as serendipity in metallo-supramolecular chemistry.[14t,56,57] Interestingly, the latter *n*-merization processes are further modulated by the ratio of the Boltzmann factors measuring the effect of the intermetallic interactions ($u_{m,n}^{\mathrm{M,M}} = e^{-(\Delta E_{m,n}^{\mathrm{M,M}}/RT)}$, Fig. 24 and 25). Due to the opposite coulombic repulsions and solvation energies contributing to $\Delta E_{m,n}^{\mathrm{M,M}}$, we can safely conclude that the final absolute values are often of limited magnitude, but it is difficult to a *priori* estimate their

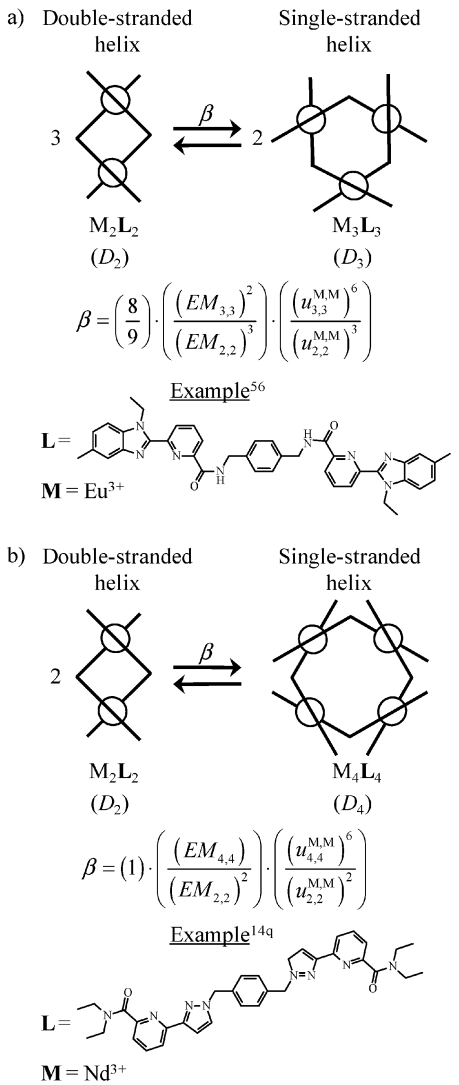

Fig. 24 Thermodynamic modeling with eqn (11) of two *n*-merization processes responsible for the destruction of standard double-helicates.

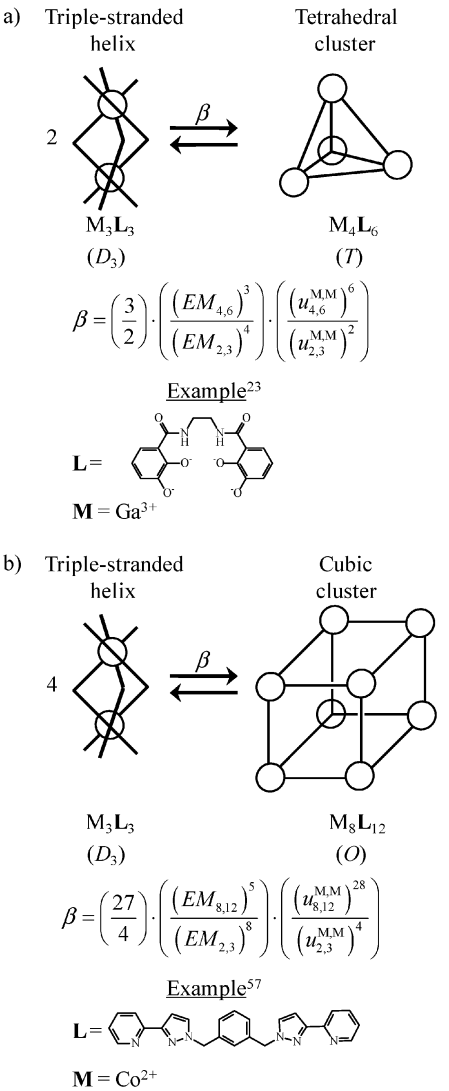

Fig. 25 Thermodynamic modeling with eqn (11) of two *n*-merization processes responsible for the destruction of standard triple-helicates.

sign. The detailed analysis of $\Delta E_{m,n}^{M,M}$ proposed for the multiple-stranded helicates obtained with the family of ligands **L7**, **L13**–**L22** indeed confirms the extreme sensitivity of this parameter to minor structural changes. We must therefore stress here that severe deviations from straightforward intuition solely based on the use of coulomb interactions, should be considered as standard trends in complicated metallo-supramolecular assemblies. Some analytical formulations for $\Delta E_{m,n}^{M,M}$ are only available for the linear helicates $[Ln_4(\mathbf{L22})_3]^{12+}$ and $[Ln_2M(\mathbf{L13})_3]^{8+}$ (eqn (62)–(66)), which strongly limits the prediction for the exact output of self-assembly processes leading to polynuclear complexes. Major efforts should be thus now extended for rationalizing and predicting intermetallic interactions operating in complexes possessing two-dimensional (Fig. 24) and three-dimensional arrays of charged cations (Fig. 25).

In conclusion, each of the five microscopic describers used in the site binding model (eqn (11)) has found a physico–chemical origin, and coordination chemists are now equipped for critically analysing their preferred self-assembly processes. Despite the extremely rough level of approximation used along this work for obtaining analytical formulations for the various describers, this approach already provides some valuable justifications concerning the design (rigidity, length, geometry) of the ligands adapted for the preparation of polynuclear complexes with variable charges, shapes, structures and stabilities.

Acknowledgements

Financial support from the Swiss National Science Foundation is gratefully acknowledged.

References and notes

1 A. Werner, *Z. Anorg. Chem.*, 1893, **3**, 267.
2 R. Abegg, *Z. Anorg. Chem.*, 1904, **39**, 330.
3 G. N. Lewis, *J. Am. Chem. Soc.*, 1916, **38**, 762.
4 (*a*) G. Schwarzenbach, *Complexometric Titrations*, Chapman & Hall, London, 1957; (*b*) F. J. Welcher, *The Analytical Uses of EDTA*, D. Van Nostrand Company, Inc., New York, 1957.
5 J. Ribas Gispert, *Coordination Chemistry*, Wiley-VCH, Weinheim, 2008.
6 L. C. Thompson, in *Handbook on the Physics and Chemistry of Rare Earths*, ed. K. A. J. Gschneidner and L. Eyring, North Holland Publ. Co. Amsterdam, 1979, ch. 25, vol. 3, p. 209.
7 (*a*) G. Schwarzenbach, *Helv. Chim. Acta*, 1952, **35**, 2344; (*b*) A. W. Adamson, *J. Am. Chem. Soc.*, 1954, **76**, 1578; (*c*) A. E. Martell, *Adv. Chem.*, 1967, **62**, 272; (*d*) D. Munro, *Chem. Br.*, 1977, **13**, 100; (*e*) E. L. Simmons, *J. Chem. Educ.*, 1979, **56**, 578; (*f*) C.-S. Chung, *J. Chem. Educ.*, 1984, **61**, 1062; R. J. Motekaitis, A. E. Martell and R. A. Hancock, *Coord. Chem. Rev.*, 1994, **133**, 39.
8 (*a*) G. Ercolani, L. Mandolini, P. Mencarelli and S. Roelens, *J. Am. Chem. Soc.*, 1993, **115**, 3901; (*b*) P. I. Kitov and D. R. Bundle, *J. Am. Chem. Soc.*, 2003, **125**, 16271; (*c*) A. Mulder, J. Huskens and D. N. Reinhoudt, *Org. Biomol. Chem.*, 2004, **2**, 3409; (*d*) D. H. Williams, E. Stephens, D. P. O'Brien and M. Zhou, *Angew. Chem., Int. Ed.*, 2004, **43**, 6596; (*e*) J. D. Badjic, A. Nelson, S. J. Cantrill, W. B. Turnbull and J. F. Stoddart, *Acc. Chem. Res.*, 2005, **38**, 723; (*f*) H.-J. Schneider and A. K. Yatsimirsky, *Chem. Soc. Rev.*, 2008, **37**, 263; (*g*) T. Rehm and C. Schmuck, *Chem. Commun.*, 2008, 801.
9 J.-M. Lehn, *Angew. Chem., Int. Ed. Engl.*, 1988, **27**, 89, and references therein.
10 C. J. Pedersen, *J. Am. Chem. Soc.*, 1967, **89**, 7017.
11 (*a*) H. K. Frensdorff, *J. Am. Chem. Soc.*, 1971, **93**, 600; (*b*) G. W. Gokel, *Crown Ethers*, Royal Society of Chemistry, Cambridge, 1990; (*c*) B. Dietrich, P. Viout and J.-M. Lehn, *Macrocyclic Chemistry: Aspects of Organic and Inorganic Supramolecular Chemistry*, VCH, Weinheim, 1993; (*d*) J.-M. Lehn, *Supramolecular Chemistry: Concepts and Perspectives*, VCH, Weinheim, 1995; (*e*) B. P. Hay and R. D. Hancock, *Coord. Chem. Rev.*, 2001, **212**, 61.
12 (*a*) J.-M. Lehn, A. Rigault, J. Siegel, J. Harrowfield, B. Chevrier and D. Moras, *Proc. Natl. Acad. Sci. U. S. A.*, 1987, **84**, 2565; (*b*) A. Pfeil and J.-M. Lehn, *J. Chem. Soc., Chem. Commun.*, 1992, 838.
13 (*a*) C. O. Dietrich-Buchecker, J. Guilhem, C. Pascard and J.-P. Sauvage, *Angew. Chem., Int. Ed. Engl.*, 1990, **29**, 1154; (*b*) G. A. Breault, C. A. Hunter and P. C. Mayers, *Tetrahedron*, 1999, **55**, 5265; (*c*) J.-P. Collin, C. Dietrich-Buchecker, C. Hamann, D. Jouvenot, J.-M. Kern, P. Mobian and J.-P. Sauvage, *Compr. Coord. Chem. II*, 2004, 303; (*d*) O. Lukin and F. Vögtle, *Angew. Chem., Int. Ed.*, 2005, **44**, 1456.
14 (*a*) E. C. Constable, *Tetrahedron*, 1992, **48**, 10013; (*b*) E. C. Constable, *Prog. Inorg. Chem.*, 1994, **42**, 67; (*c*) D. S. Lawrence, T. Jiang and M. Levett, *Chem. Rev.*, 1995, **95**, 2229; (*d*) D. Philp and J. F. Stoddart, *Angew. Chem., Int. Ed. Engl.*, 1996, **35**, 1154; (*e*) C. Piguet, G. Bernardinelli and G. Hopfgartner, *Chem. Rev.*, 1997, **97**, 2005; (*f*) C. Piguet, *J. Inclusion Phenom. Macrocyclic Chem.*, 1999, **34**, 361; (*g*) D. L. Caulder and K. N. Raymond, *Acc. Chem. Res.*, 1999, **32**, 975; (*h*) S. Leininger, B. Olenyuk and P. J. Stang, *Chem. Rev.*, 2000, **100**, 853; (*i*) G. F. Swiegers and T. J. Malefetse, *Chem. Rev.*, 2000, **100**, 3483; (*j*) M. Fujita, K. Umemoto, M. Yoshizawa, N. Fujita, T. Kusukawa and K. Biradha, *Chem. Commun.*, 2001, 509; (*k*) G. F. Swiegers and T. J. Malefetse, *J. Inclusion Phenom. Macrocyclic Chem.*, 2001, **40**, 253; (*l*) M. Albrecht, *Chem. Rev.*, 2001, **101**, 3457; (*m*) P. D. Beer and E. J. Hayes, *Coord. Chem. Rev.*, 2003, **240**, 167; (*n*) M. Fujita, M. Tominaga, A. Hori and B. Therrien, *Acc. Chem. Res.*, 2005, **38**, 369; (*o*) V. Maurizot, M. Yoshizawa, M. Kawano and M. Fujita, *Dalton Trans.*, 2006, 2750; (*p*) E. R. Kay, D. A. Leigh and F. Zerbetto, *Angew. Chem., Int. Ed.*, 2007, **46**, 72; (*q*) T. K. Ronson, H. Adams, L. P. Harding, S. J. A. Pope, D. Sykes, S. Faulkner and M. D. Ward, *Dalton Trans.*, 2007, 1006; (*r*) R. W. Saalfrank, H. Maid and A. Scheurer, *Angew. Chem., Int. Ed.*, 2008, **47**, 8794; (*s*) B. H. Northrop, Y.-R. Zheng, K.-W. Chi and P. J. Stang, *Acc. Chem. Res.*, 2009, **42**, 1554; (*t*) M. D. Ward, *Chem. Commun.*, 2009, 4487.
15 (*a*) N. Fatin-Rouge, S. Blanc, E. Leize, A. van Dorsselaer, P. Baret, J.-L. Pierre and A. M. Albrecht-Gary, *Inorg. Chem.*, 2000, **39**, 5771; (*b*) N. Fatin-Rouge, S. Blanc, A. Pfeil, A. Rigault, A.-M. Albrecht-Gary and J.-M. Lehn, *Helv. Chim. Acta*, 2001, **84**, 1694; (*c*) J. Hamacek, S. Blanc, M. Elhabiri, E. Leize, A. van Dorsselaer, C. Piguet and A. M. Albrecht-Gary, *J. Am. Chem. Soc.*, 2003, **125**, 1541; (*d*) M. Elhabiri, J. Hamacek, J.-C. G. Bünzli and A. M. Albrecht-Gary, *Eur. J. Inorg. Chem.*, 2004, 51; (*e*) M. Elhabiri, J. Hamacek, N. Humbert, J.-C. G. Bünzli and A. M. Albrecht-Gary, *New J. Chem.*, 2004, **28**, 1096; (*f*) M. Elhabiri and A. M. Albrecht-Gary, *Coord. Chem. Rev.*, 2008, **252**, 1079.
16 (*a*) G. Ercolani, *J. Am. Chem. Soc.*, 2003, **125**, 16097; (*b*) G. Ercolani, *J. Phys. Chem. B*, 2003, **107**, 5052.
17 J. Hamacek and C. Piguet, *J. Phys. Chem. B*, 2006, **110**, 7783.
18 (*a*) M. Borkovec, J. Hamacek and C. Piguet, *Dalton Trans.*, 2004, 4096; (*b*) J. Hamacek, M. Borkovec and C. Piguet, *Chem.–Eur. J.*, 2005, **11**, 5217; (*c*) J. Hamacek, M. Borkovec and C. Piguet, *Chem.–Eur. J.*, 2005, **11**, 5227; (*d*) M. Borkovec, G. J. M. Koper and C. Piguet, *Curr. Opin. Colloid Interface Sci.*, 2006, **11**, 280.
19 C. Piguet, M. Borkovec, J. Hamacek and K. Zeckert, *Coord. Chem. Rev.*, 2005, **249**, 705.
20 T. M. Fyles and C. C. Tong, *New J. Chem.*, 2007, **31**, 296.
21 (*a*) C. A. Hunter and S. Tomas, *J. Am. Chem. Soc.*, 2006, **128**, 8975; (*b*) E. Chekmeneva, C. A. Hunter, M. J. Packer and S. M. Turega, *J. Am. Chem. Soc.*, 2008, **130**, 17718; (*c*) C. A. Hunter and H. L. Anderson, *Angew. Chem., Int. Ed.*, 2009, **48**, 7488; (*d*) A. Camara-Campos, D. Musumeci, C. A. Hunter and S. Turega, *J. Am. Chem. Soc.*, 2009, **131**, 18518.
22 J. Hamacek, M. Borkovec and C. Piguet, *Dalton Trans.*, 2006, 1473.

23 (*a*) E. J. Enemark and T. D. P. Stack, *Inorg. Chem.*, 1996, **35**, 2719; (*b*) E. J. Enemark and T. D. P. Stack, *Angew. Chem., Int. Ed.*, 1998, **37**, 932.
24 G. Ercolani, C. Piguet, M. Borkovec and J. Hamacek, *J. Phys. Chem. B*, 2007, **111**, 12195.
25 L. Mandolini, *Adv. Phys. Org. Chem.*, 1987, **22**, 1.
26 R. E. Powell and W. M. Latimer, *J. Chem. Phys.*, 1951, **19**, 1139.
27 (*a*) W. Kuhn, *Kolloid-Z.*, 1934, **68**, 2; (*b*) H. Jacobson and W. H. Stockmayer, *J. Chem. Phys.*, 1950, **18**, 1600; (*c*) P. J. Flory, U. W. Suter and M. Mutter, *J. Am. Chem. Soc.*, 1976, **98**, 5733; (*d*) W. P. Jencks, *Proc. Natl. Acad. Sci. U. S. A.*, 1981, **78**, 4046; (*e*) M. A. Winnik, *Chem. Rev.*, 1981, **81**, 491; (*f*) X. Chi, A. J. Guerin, R. A. Haycock, C. A. Hunter and L. D. Sarson, *J. Chem. Soc., Chem. Commun.*, 1995, 2563; (*g*) G. Ercolani, *J. Phys. Chem. B*, 1998, **102**, 5699; (*h*) R. H. Kramer and J. W. Karpen, *Nature*, 1998, **395**, 710; (*i*) C. Galli and L. Mandolini, *Eur. J. Org. Chem.*, 2000, 3117; (*j*) J. M. Gargano, T. Ngo, J. Y. Kim, D. W. K. Acheson and W. J. Lees, *J. Am. Chem. Soc.*, 2001, **123**, 12909.
28 It is worth mentioning here that the associated free energy term $\Delta g^{M,L}_{preorg} = -RT\ln(EM^{M,L})$ has been recently referred to as 'chelate cooperativity' by Hunter and Anderson,[21c] which could bring some regrettable confusion because the latter term simply corresponds to the advantage (or disadvantage) of the intramolecular connection, but does not involve its variation during the thermodynamic self-assembly process, a change which is required for a non-zero contribution to the cooperativity of the assembly process.
29 In reference to the protein–ligand model, which attributes the origin of the allosteric effect to the homo-component corrections,[17] Hunter and Anderson used the term 'allosteric cooperativity' for the contribution of the latter parameters to the total free energy change $\Delta G_{homo} = \sum_i \Delta E_i^{M,M} + \sum_j \Delta E_j^{L,L}$[21c].
30 D.-M. Bishop and K. J. Laidler, *J. Chem. Phys.*, 1965, **42**, 1688.
31 (*a*) S. W. Benson, *J. Am. Chem. Soc.*, 1958, **80**, 5151; (*b*) W. F. Bailey and A. S. Monahan, *J. Chem. Educ.*, 1978, **55**, 489.
32 J.-C. G. Bünzli and A. Milicic-Tang, in *Handbook on the Physics and Chemistry of Rare Earths*, ed. K. A. Gschneidner and L. Eyring, North Holland Publ. Co., Amsterdam, 1995, vol. 21, p. 305.
33 A. Escande, L. Guénée, K.-L. Buchwalder and C. Piguet, *Inorg. Chem.*, 2009, **48**, 1132.
34 N. Dalla Favera, L. Guénée, G. Bernadinelli and C. Piguet, *Dalton Trans.*, 2009, 7625.
35 (*a*) G. R. Choppin, in *Lanthanide Probes in Life, Chemical and Earth Sciences*, ed. J.-C. G. Bünzli and G. R. Choppin, Elsevier, Amsterdam, 1989, ch. 1; (*b*) C. Piguet and J.-C. G. Bünzli, *Chem. Soc. Rev.*, 1999, **28**, 347.
36 G. Canard, S. Koeller, G. Bernardinelli and C. Piguet, *J. Am. Chem. Soc.*, 2008, **130**, 1025.
37 When discussing the theoretical concept, the effective molarity is often referred to as the effective concentration. For the sake of clarity in this feature article, we will use the term effective molarity, *EM*, for both the theoretical concept and its experimental value (see ref. 8*c* for more details).
38 N. Dalla Favera, J. Hamacek, M. Borkovec, D. Jeannerat, F. Gumy, J.-C. G. Bünzli, G. Ercolani and C. Piguet, *Chem.–Eur. J.*, 2008, **14**, 2994.
39 G. Ercolani, *Struct. Bonding*, 2006, **121**, 167, and references therein.
40 I. Grenthe, *J. Am. Chem. Soc.*, 1961, **83**, 360.
41 We consider the aquo ions $[Ln(H_2O)_9]^{3+}$ as D_{3h} tricapped trigonal prismatic complexes along the complete lanthanide series despite the well-established change from $CN = 9$ to $CN = 8$ near the middle of the series. A more elaborate calculation of the statistical factors taking into account this change only slightly affects the fitted values of $\Delta g^{Ln,L8}_{inter}$ and $\Delta E^{L8,L8}$.
42 G. Canard and C. Piguet, *Inorg. Chem.*, 2007, **46**, 3511.
43 E. O. Purisima and T. Sulea, *J. Phys. Chem. B*, 2009, **113**, 8206.
44 S. Torelli, S. Delahaye, A. Hauser, G. Bernardinelli and C. Piguet, *Chem.–Eur. J.*, 2004, **10**, 3503.
45 M. Cantuel, G. Bernardinelli, D. Imbert, J.-C. G. Bünzli, G. Hopfgartner and C. Piguet, *J. Chem. Soc., Dalton Trans.*, 2002, 1929.
46 (*a*) M. Born, *Z. Phys.*, 1920, **1**, 45; (*b*) B. E. Conway, in *Modern Aspects of Electrochemistry*, ed. B. E. Conway and R. E. White, Kluwer Academic/Plenum Publishers, 2002, pp. 295–323; (*c*) R. H. Stokes, *J. Phys. Chem.*, 1964, **86**, 979; (*d*) T. Abe, *Bull. Chem. Soc. Jpn.*, 1991, **64**, 3035; (*e*) A. Kumar, *J. Phys. Soc. Jpn.*, 1992, **61**, 4247.
47 T. Riis-Johannessen, N. Dalla Favera, T. K. Todorova, S. M. Huber, L. Gagliardi and C. Piguet, *Chem.–Eur. J.*, 2009, **15**, 12702.
48 (*a*) M. Albrecht, *Chem.–Eur. J.*, 1997, **3**, 1466; (*b*) M. Albrecht, M. Schneider and H. Röttele, *Angew. Chem., Int. Ed.*, 1999, **38**, 557.
49 (*a*) D. W. Johnson and K. N. Raymond, *Inorg. Chem.*, 2001, **40**, 5157; (*b*) A. V. Davis and K. N. Raymond, *J. Am. Chem. Soc.*, 2005, **127**, 7912; (*c*) A. V. Davis, D. Fiedler, G. Seeber, A. Zahl, R. van Eldik and K. N. Raymond, *J. Am. Chem. Soc.*, 2006, **128**, 1324.
50 (*a*) U. Kiehne, T. Weilandt and A. Lützen, *Org. Lett.*, 2007, **9**, 1283; (*b*) N. Dalla Favera, U. Kiehne, J. Bunzen, S. Hyteballe, A. Lützen and C. Piguet, *Angew. Chem., Int. Ed.*, 2010, **49**, 125.
51 A. E. Martell and R. M. Smith, *Critical Stability Constants*, Plenum Press, New York, 1982, vol. 4–5.
52 E. Terazzi, L. Guénée, B. Bocquet, J.-F. Lemonnier, N. Dalla Favera and C. Piguet, *Chem.–Eur. J.*, 2009, **15**, 12719.
53 J.-F. Lemonnier, L. Guénée, G. Bernardinelli, J.-F. Vigier, B. Bocquet and C. Piguet, *Inorg. Chem.*, 2010, **49**, 1252.
54 (*a*) M. S. Searle and D. H. Williams, *J. Am. Chem. Soc.*, 1992, **114**, 10690; (*b*) M. S. Searle, M. S. Westwell and D. H. Williams, *J. Chem. Soc., Perkin Trans. 2*, 1995, 141; (*c*) D. H. Williams, D. P. O'Brien and B. Bardsley, *J. Am. Chem. Soc.*, 2001, **123**, 737; (*d*) A. A. Levchenko, C. K. Yee, A. N. Parikh and A. Navrotsky, *Chem. Mater.*, 2005, **17**, 5428; (*e*) D. M. Ford, *J. Am. Chem. Soc.*, 2005, **127**, 16167.
55 M. I. Page and W. P. Jencks, *Proc. Natl. Acad. Sci. U. S. A.*, 1971, **68**, 1678. For a bimolecular reaction in solution, the change in translational entropy corresponds to about 146 J mol^{-1} K^{-1} based on a standard state of 1 m.
56 J.-M. Senegas, S. Koeller and C. Piguet, *Chem. Commun.*, 2005, 2235.
57 A. M. Najar, I. S. Tidmarsh and M. D. Ward, *Inorg. Chem.*, 2009, **48**, 11871.